



# Non-additive phospholipidomic responses to ocean warming and acidification drive intraspecific variation in cell membrane vulnerability in a marine ectotherm

Lauric Feugere<sup>a,\*</sup>, Joana Filipa Fernandes<sup>a,b</sup>, Ella Guscelli<sup>a</sup>, Tânia Melo<sup>c,d</sup>, Susana Aveiro<sup>c,d</sup>, Denis Chabot<sup>e</sup>, Ricardo Calado<sup>b</sup>, Rosário Domingues<sup>c,d</sup>, Diana Madeira<sup>b</sup>, Piero Calosi<sup>a</sup>

<sup>a</sup> Marine Ecological and Evolutionary Physiology (MEEP) Laboratory, Département de Biologie, Chimie et Géographie, Université du Québec à Rimouski, 300 Allée des Ursulines, Rimouski, QC, G5L 3A1, Canada

<sup>b</sup> ECOMARE & CESAM & Department of Biology, University of Aveiro, Campus Universitário de Santiago, Aveiro, Portugal

<sup>c</sup> Mass Spectrometry Centre, LAQV-REQUIMTE, Department of Chemistry, University of Aveiro, Santiago University Campus, 3810-193 Aveiro, Portugal

<sup>d</sup> CESAM-Centre for Environmental and Marine Studies, Department of Chemistry, University of Aveiro, Aveiro, Portugal

<sup>e</sup> Institut Maurice-Lamontagne, Pêches et Océans Canada, Mont-Joli, QC, Canada

## ARTICLE INFO

Handling editor: Robert Letcher

### Keywords:

Synergism  
Antagonism  
Adaptation  
Acclimatisation  
Lipidome  
Cellular vulnerability  
Marine invertebrates

## ABSTRACT

The lipidome is fundamental to the good functioning of cells and organisms. However, its role in species acclimatisation and adaptation to global changes remains overlooked. Investigating intraspecific variation in lipidome responses to combined global change drivers is therefore paramount to predict species' vulnerability in future oceans. Here, we profiled the phospholipidome of the Northern shrimp, *Pandalus borealis*, from four different origins in the Northwest Atlantic, within an orthogonal design of ocean warming (OW) and acidification (OA) scenarios. We report complex origin-dependent non-additive responses under combined global changes. Shrimp display a high degree of intraspecific variation with distinct profiles of synergism, antagonism or temperature-driven phospholipidome responses when OA is superimposed on OW. Shrimp from the southernmost origin are only sensitive to OW, whilst those from the other three origins respond to combined OW and OA. These patterns involve changes in cellular membranes' unsaturation, fluidity, curvature and thickness, underlying differential intraspecific cellular vulnerability to global changes. The isolated effects of OA are subtler, visible only in shrimp from the St. Lawrence Estuary (SLE). Shrimp from SLE also show the most pronounced phospholipidome remodelling, allowing them to acclimate to combined OW and OA. Whilst SLE shrimp seem most sensitive to global changes, those from the northernmost origins (Newfoundland and Esquiman Channel) display the greatest cellular vulnerability under combined OW and OA. Our findings evidence the highly complex interplay of OW and OA in remodelling marine ectotherms' phospholipidomes, with direct implications for prioritising conservation efforts on populations most vulnerable to global changes.

## 1. Introduction

The lipidome comprises all lipids in a biological system (Han and Gross, 2003, 2022). These lipids are involved in cell membrane structuring, energy storage, signalling and immunity, making them central to the functioning of all life forms (Johnson et al., 2021; Trautenberg et al., 2022; Xianlin, 2016). However, the architectural organisation and

functioning of the lipidome, particularly in marine non-model organisms, remains poorly studied (Koelmel et al., 2020). Phospholipids, also known as glycerophospholipids, the main lipids in cells, have amphiphilic properties allowing them to form and regulate cellular and sub-cellular membrane bilayers (Liebisch et al., 2020; Lordan et al., 2017). Particularly, the composition of phospholipids dictates the fluidity, curvature and thickness of cellular membranes, in turn controlling their

\* Corresponding author.

E-mail addresses: [Lauric.Feugere@uqar.ca](mailto:Lauric.Feugere@uqar.ca) (L. Feugere), [joanafcf@ua.pt](mailto:joanafcf@ua.pt) (J.F. Fernandes), [Ella.Guscelli@uqar.ca](mailto:Ella.Guscelli@uqar.ca) (E. Guscelli), [taniamelo@ua.pt](mailto:taniamelo@ua.pt) (T. Melo), [s.aveiro@ua.pt](mailto:s.aveiro@ua.pt) (S. Aveiro), [chabot.denis@gmail.com](mailto:chabot.denis@gmail.com) (D. Chabot), [rjcalado@ua.pt](mailto:rjcalado@ua.pt) (R. Calado), [mrd@ua.pt](mailto:mrd@ua.pt) (R. Domingues), [d.madeira@ua.pt](mailto:d.madeira@ua.pt) (D. Madeira), [Piero.Calosi@uqar.ca](mailto:Piero.Calosi@uqar.ca) (P. Calosi).

<https://doi.org/10.1016/j.envres.2025.122135>

Received 28 March 2025; Received in revised form 8 June 2025; Accepted 10 June 2025

Available online 11 June 2025

0013-9351/© 2025 The Authors. Published by Elsevier Inc. This is an open access article under the CC BY license (<http://creativecommons.org/licenses/by/4.0/>).

integrity and associated functions (Falch, 2023; Lischka et al., 2022; Lordan et al., 2017). Ultimately, phospholipids have broader ecological roles cascading through trophic networks (Trautenberg et al., 2022), and provide key health-promoting benefits to human consumption (Bergé and Barnathan, 2005; Falch, 2023).

Lipidomic approaches can help to acquire a more comprehensive understanding of the mechanisms underpinning organisms' vulnerability to global changes (Han and Gross, 2022; Imbs et al., 2021; Rey et al., 2022). This is particularly critical for marine organisms, which are becoming increasingly important as a food source with accelerating human demographics, with the food industry and food security being challenged by global changes (Costello et al., 2020; FAO, 2024). Amidst major global change drivers, ocean warming (OW) will increase the global ocean temperature by 4 °C by 2100 and 8 °C by 2300 (scenario RCP 8.5, Horton et al., 2020; IPCC, 2022). Simultaneously, ocean acidification (OA) caused by anthropogenic CO<sub>2</sub> injections in the atmosphere is progressively disrupting the seawater carbonate system and will lower the seawater pH by -0.3 units by 2100 (Caldeira and Wickert, 2003; Doney et al., 2009; IPCC, 2022). In isolation, both OW (Ermolenko and Sikorskaya, 2021; Facchini et al., 2016; Sikorskaya et al., 2020) and OA (Lischka et al., 2022) were shown to cause a lipidome rewiring in marine invertebrates. This generally involves membrane composition adjustments such as its unsaturation levels, whilst lipid classes and chain length can also be modulated but usually remain more stable (Chwastek et al., 2020; Ernst et al., 2016, 2018). For instance, organisms increase or decrease cellular membrane levels of unsaturated lipids, respectively, when exposed to colder or warmer temperatures to maintain membranes' fluidity (Holm et al., 2022; Ohtsu et al., 1998; Sinensky, 1974). In contrast, adaptation to OA may involve higher unsaturation levels to limit cell permeability to CO<sub>2</sub> and regulate cell homeostasis (Jin et al., 2021). However, multiple stressors can interact with each other and exert complex non-additive responses, such as antagonisms and synergisms (Carrier-Belleau et al., 2021; Côté et al., 2016; Piggott et al., 2015). Few studies to date have characterised the combined effects of OW and OA on the lipid profiles of metazoans, with most research focusing on total lipid content and fatty acid profiles (Lischka et al., 2022). These studies report that temperature acts as the major driver of lipid composition, whilst OA has more subtle effects (Garzke et al., 2016; Lischka et al., 2022; Rivest and Hofmann, 2015; Schoepf et al., 2013). Nonetheless, combined OW and OA may lower the prevalence of polyunsaturated fatty acids or accentuate declines in total lipids in marine metazoans (Lischka et al., 2022; Valles-Regino et al., 2015). However, it remains unknown how the remodelling of the phospholipidome will help mediate marine species' success and evolutionary trajectories under changing environments.

Within the context of global changes, it is paramount to characterise intraspecific molecular variation between organisms inhabiting distinct regional environments to better predict populations' and species' vulnerabilities to ongoing global changes (Calosi et al., 2017; Guscelli et al., 2023a; Meek et al., 2023; Schmidt and Donelson, 2024). However, the prevalence of such large-scale intraspecific variation remains neglected at the lipidome level. The broad range of functions regulated by lipids and our poor critical understanding of their responses to global changes highlight the urgent need to assess whether functional lipidomics can be used as a tool to support the conservation of marine species in future oceans (Han and Gross, 2022; Rey et al., 2022; Wood et al., 2023). Particularly, recent advancements in lipid functional annotation and ontology facilitate the interpretation of lipidomics into biological insights (Kyle et al., 2021; Molenaar et al., 2019), allowing us to better understand how aquatic organisms respond to environmental challenges (Cho et al., 2022; Eide et al., 2023; Fuertes et al., 2020; Mesmar et al., 2024).

Here, we compare for the first time the phospholipidome responses of multiple populations of a marine ectotherm to the combined exposure to OW and OA. For this purpose, we used the Northern shrimp *Pandalus borealis* (Krøyer, 1838) as an ideal study species known to be sensitive to

these drivers in isolation and combined at both the metabolome and whole-organism levels (Chemel et al., 2020; Guscelli et al., 2023a, 2023b). The Northern shrimp is a major high-commercial and cultural value crustacean, its worldwide production averaging 280,000 tons per year between 2010 and 2019 (DFO, 2024; FAO, 2022; Gillett, 2008). For instance, in Canada, landings averaged 339 M\$ CAD yearly in the period 2008–2023 (DFO, 2025). However, in the Northwest Atlantic, Northern shrimp populations are currently declining, particularly at the southern edge of this species' geographical distribution, in part due to OW (Baker et al., 2024; DFO, 2022a, 2022b, 2021; Richards and Hunter, 2021), with possible drastic ecological and economic repercussions. The Northern shrimp is potentially locally adapted to recent changes in regional seawater temperatures (Bouret et al., 2024; Ouellet et al., 2017), whilst we know less of its adaptive capacity to OA. Guscelli et al. (2023a, 2023b) reported that Northern shrimp from different geographic origins show comparable low survival rates and metabolic performance when exposed to combined OW and OA, but display different metabolomic strategies, emphasising the crucial need to investigate multiple biological layers to define an organisms' sensitivity to environmental challenges (Bartholomew, 1986; Madeira et al., 2024). At the phospholipidome level, we anticipate functional changes in Northern shrimp from different origins to help identify regions of concern for prioritising stock conservation strategies. We expect that the phospholipidome of shrimp will respond differently to a combined exposure of OW and OA, as their regions of origin feature different environmental conditions. Although we expect temperature to be the major driver based on prior evidence, we hypothesise the emergence of non-additive (*i.e.*, interaction) phospholipidome responses to OW and OA, and specifically synergistic (*sensu* Côté et al., 2016). The abdominal muscle plays a key role in swimming, for example, to escape predators (Robles-Romo et al., 2016). In addition, the abdominal muscle is important in storing phospholipids in crustaceans, critically influencing their survival under environmental stressors (Mika et al., 2013; Perez-Velazquez et al., 2003) and determining their trophic, nutritional and commercial values (Chemel et al., 2020; Latyshev et al., 2009; Wan et al., 2022; Yu et al., 2020). Therefore, to test these hypotheses, we performed untargeted phospholipidomics on the abdominal muscle of female shrimp from four distinct origins in the Northwest Atlantic following a 30-day exposure to single and combined OW and OA scenarios, according to a fully replicated orthogonal experimental design (Fig. S1A).

## 2. Materials and methods

### 2.1. Specimen collection and experimental design

Tissue samples used to characterise the phospholipidome responses of the abdominal muscle of females of the Northern shrimp *Pandalus borealis* to OW and OA were obtained from specimens exposed under laboratory conditions to these global change drivers for 30 d from the study by Guscelli and collaborators (see Chemel et al., 2020; Guscelli, 2024; Guscelli et al., 2023a,b, 2024, for details on experimental conditions and shrimp collection). Briefly, shrimp were collected with shrimp trawls or traps from four different geographic origins in the Northwest Atlantic: St. Lawrence Estuary (SLE, 48° 35' N, 68° 35' W in May 2018), Esquiman Channel (EC, 50° 44' N, 57° 29' W in July 2019), Eastern Scotian Shelf (ESS, 45° 23' N, 61° 04' W in February 2019) and Northeast Newfoundland Coast (NNC, 50° 18' N, 54° 16' W; November 2019; see Fig. S1A and Guscelli et al., 2023b). Conditions of temperature, pH and dissolved oxygen saturation (DO) at the different sampling points were retrieved from mission reports and published literature on environmental monitoring at the nearest locations for SLE (120–140 m, ~3 °C, ~60 % DO, pH ~7.8), EC (250 m, ~6.5 °C, <30 % DO, pH ~7.6), ESS (~100 m, ~2.3 °C, >80 % DO, pH ~7.9–8), and NNC (270 m, ~2.5 °C, >80 % DO, pH ~8) (Bourdages et al., 2022; DFO, 2020; Drozdowski and Horne, 2022; Gibb et al., 2023; Koeller et al., 2007; Mucci et al., 2011).

See Guscelli (2024) for further details on origin-specific environmental conditions. We chose female shrimp as they are the main target of fisheries and more sensitive than males to global changes (DFO, 2016; Dupont-Prinet et al., 2013). Shrimp from each origin were kept under laboratory conditions for ~8 weeks before the experiment started. Although we acknowledge the possible influence of seasonality, as shrimp from different origins were collected at different times, this effect was mitigated as much as possible by this 8-week-long pre-exposure to stable environmental conditions and diet, which were similar across origins. During the acclimation period, shrimp were maintained in seawater pumped 2 km offshore of the facilities, and temperature and salinity were controlled to an average temperature of 4.5 °C and an average salinity of 32, whereas pH was naturally around 7.9. Shrimp were fed *ad libitum* a mix of capelin and shrimp during the experimental exposure as described in Chemel et al. (2020). Methods regarding the regulation and monitoring of seawater parameters during the experimental exposure are described in Chemel et al. (2020) and Guscelli et al. (2023b). The seawater parameters during the experimental exposure are provided as Supplementary Table S1 in Guscelli et al. (2023b) and on the PANGAEA - Data Publisher for Earth & Environmental Sciences (Guscelli et al., 2024). Briefly, adding salt, automatically injecting hot/cold sea water via a temperature controller and automatically adding pure gaseous CO<sub>2</sub> enabled us to regulate salinity, temperature and pH conditions during the experimental exposure, respectively. Shrimp were then exposed for 30 days to a quadratic design of end-of-century OW and OA conditions combining three temperatures (2, 6, 10 °C) and two pH (pH 7.75 and pH 7.40) levels (See Fig. S1A). We opted for (i) 2 °C as a favourable condition for shrimp and as the lower limit of their preferred temperature range of 2–4 °C (Baker et al., 2024) (ii) 6 °C as near-future oceanic conditions under a +4 °C global temperature (IPCC, 2022), but still in the permissive temperature range of shrimp (Garcia, 2007); and (iii) 10 °C as a temperature near shrimp's upper thermal limits towards 12 °C (Shumway, 1985), close to the upper temperature of 9.2 °C at which shrimp are found in the area (Baker et al., 2024) and as future oceanic conditions under a global +8 °C scenario by 2300 (Horton et al., 2020; IPCC, 2022). A pH of 7.75 represented current conditions for shrimp originating from inside the Gulf of St. Lawrence (Mucci et al., 2011, 2018), whilst 7.40 mimicked a -0.3 pH unit decrease (IPCC, 2022). The six experimental treatments (~70 shrimp per individual treatment with two replicate tanks per treatment) were as follows: 2 °C/pH 7.75 (2C, considered as the favourable condition to which other treatments were compared), 6 °C/pH 7.75 (6C), 10 °C/pH 7.75 (10C), 2 °C/pH 7.40 (2A), 6 °C/pH 7.40 (6A) and 10 °C/pH 7.40 (10A). This allowed us to compare the effects of combined OW and OA in either a 6 °C or 10 °C scenario. In order to obtain muscle samples to estimate the effects of OW and OA on phospholipidome profiles, ten shrimp per treatment (five shrimp per tank) were rapidly dissected on ice at the end of the experimental exposure and following respirometry trials described in Guscelli et al. (2023b). Abdominal muscle samples were placed in microtubes and flash-frozen in liquid nitrogen and preserved at -80 °C before being dried-shipped in nitrogen to the Centre for Environmental and Marine Studies (Aveiro, Portugal), where they were processed for phospholipidomics at ECOMARE facilities (Laboratory for Innovation and Sustainability of Marine Biological Resources) and Mass Spectrometry Centre of the University of Aveiro (Portugal).

## 2.2. LC-MS/MS phospholipidomics

### 2.2.1. Preparation of abdominal tissue samples from female shrimp

Tissue samples (approx. 100 mg) were freeze-dried (freeze-dryer CoolSafe Pro -55 °C 9 L from Frilabo®) for 3 d, before sample homogenisation and phospholipid extraction. For this purpose, dried tissues were ground using a ceramic mortar and pestle and preserved at -80 °C until further processing.

### 2.2.2. Phospholipid extraction

Phospholipids in abdominal tissue samples of female shrimp were extracted according to the modified Bligh and Dyer method (Bligh and Dyer, 1959). Briefly, approximately 50 mg of freeze-dried shrimp samples were weighed on an analytical scale (ADA 180, ADAM, Oxford, UK) in 10 mL glass tubes with tight screw caps (PYREX SVL 15,100 × 16 mm, Darmstadt, Germany). Next, 2.5 mL of methanol (CH<sub>3</sub>OH, Fisher Scientific Ltd., Loughborough, UK) and 1.25 mL of dichloromethane (CH<sub>2</sub>Cl<sub>2</sub>, Fisher Scientific Ltd., Loughborough, UK) was added to the glass tubes, which were vortexed (1 min), sonicated (1 min) and incubated on ice for 30 min. The glass tubes were vortexed again and centrifuged (Selecta JP Mixtasel, Abrera, Barcelona, Spain) for 10 min at 626 g at room temperature. The supernatant was collected into a second glass tube and a volume of 2.5 mL of dichloromethane and 1.25 mL of ultrapure water (Synergy, Millipore Corporation, Billerica, MA, USA) was added to the tubes, resolving a two-phase system. Samples were then centrifuged again (Selecta JP Mixtasel, Abrera) at 626 g for 10 min at room temperature and the lower organic phase was collected into a new glass tube. To limit the loss of phospholipid during the extraction, another 1.88 mL of dichloromethane was added to the remaining aqueous phase, which was vortexed and centrifuged (Selecta JP Mixtasel, Abrera) another time. The organic phases were collected together and evaporated under a nitrogen stream until completely dry.

Following this step, 0.4 mL of dichloromethane was added to the tubes and vortexed to dissolve the phospholipids, which were then transferred to amber vials. These vials were previously dried in an oven at 105 °C for 2 h to remove traces of humidity and weighed with an analytical scale (ADA 180, ADAM). The tubes were rinsed with another 0.5 mL of dichloromethane before transferring it to the vials to reach a total volume of 0.9 mL. The reconstituted phospholipids were dried in the vial under a nitrogen stream and subsequently weighed to determine the amount of phospholipid extract (see Supplementary Methods for more details on the phospholipid quantification) by gravimetry using an analytical scale (ADA 180, ADAM). Vials were stored at -20 °C until phospholipids were quantified. Samples were extracted in six batches of ~40+ samples per batch, with treatments being randomised and alternated for LC-MS/MS.

### 2.2.3. Analysis of phospholipids using high-resolution LC-MS and MS/MS

An untargeted phospholipidomics approach was used to evaluate the stability of the phospholipidome across populations and treatment conditions. This approach provided a global profile of the phospholipid molecular species present in the shrimp extracts. For this purpose, the phospholipid extracts were analysed by hydrophilic interaction liquid chromatography (HILIC) on a liquid chromatograph (Ultimate 3000 Dionex, Thermo Fisher Scientific, Bremen, Germany) with an autosampler coupled to a mass spectrometer (Q-Exactive hybrid quadrupole, Thermo Fisher, Scientific, Bremen, Germany). Mobile phase A consisted of 25 % water, 50 % acetonitrile and 25 % MeOH, with 5 mM ammonium acetate and mobile phase B consisted of 60 % acetonitrile and 40 % MeOH, with the same amount of ammonium acetate in mobile phase A. The solvent gradient, flow rate through column and conditions used for acquisition of full scan LC-MS spectra and LC-MS/MS spectra in both positive and negative ion modes were the same as previously described (da Costa et al., 2015; Melo et al., 2015). Initially, 40 % of mobile phase A was held isocratically for 8 min, followed by a linear increase to 60 % of mobile phase A within 7 min and a maintenance period of 5 min, returning to the initial conditions in 15 min (5 min to return to 40 % of mobile phase A and a re-equilibration period of 10 min). For each phospholipid extract, the amount of total phospholipid was quantified (mean ± SE: 3.67 ± 0.031 mg) following the molybdovanadate method (see Supplementary Methods for more details on the phospholipid quantification). This allowed the injection of a standardised amount of 10 µg of each phospholipid extract, corresponding to a volume of 10 µL in CH<sub>2</sub>Cl<sub>2</sub>, mixed with 82 µL of eluent B. Then, 8 µL of phospholipid standards mix (see Table S1), purchased from Avanti Polar Lipids, Inc.

(Alabaster, AL, USA), was added to each sample. Further, 5  $\mu\text{L}$  of each previously diluted sample was introduced into the Ascentis Si column (15 cm  $\times$  1 mm, 3  $\mu\text{m}$ , Sigma-Aldrich, Darmstadt, Germany) with a flow rate of 40  $\mu\text{L min}^{-1}$  at 30  $^{\circ}\text{C}$ . The mass spectrometer with Orbitrap® technology was operated in simultaneous positive (electrospray voltage 3.0 kV) and negative (electrospray voltage – 2.7 kV) modes with high resolution with 70,000 and AGC target of  $1 \times 10^6$ , the capillary temperature was 250  $^{\circ}\text{C}$  and the sheath gas flow was 15 U.

For MS/MS analysis, a resolution of 17,500 and AGC target of  $1 \times 10^5$  were used and the cycles consisted of one full scan mass spectrum and ten data-dependent MS/MS scans were repeated continuously throughout the experiments with the dynamic exclusion of 60 s and intensity threshold of  $2 \times 10^4$ . Normalised collision energy™ (CE) ranged between 25, 30 and 35 eV. Data acquisition was performed using the Xcalibur data system (V3.3, Thermo Fisher Scientific, USA). The identification of molecular species of phospholipids was based on the assignment of the molecular ions observed in LC-MS spectra, typical retention time, mass accuracy and LC-MS/MS spectra manual analysis that allowed confirming the identity of the polar head group and the fatty acyl chains for most of the molecular species.

### 2.3. Statistical analyses

We identified 269 phospholipids, quantified their peak areas, standardised data to the peak area of internal standards with a known injected mass (see [Supplementary Table S1](#)) and transformed data via an ordered quantile normalisation (see [Supplementary Methods](#) for details). We investigated and reported the effects of Origin, OW and OA on the phospholipidome following the language of evidence proposed by [Muff et al. \(2022\)](#) as little/none ( $P > 0.1$ ), weak ( $P < 0.1$ ), moderate ( $P < 0.05$ ), strong ( $P < 0.01$ ) and very strong ( $P < 0.001$ ). In order to explore possible non-additive (*i.e.*, interaction) effects between OW and OA within each origin and warming scenario, we compared the phospholipidome profiles of shrimp exposed to single and combined OW and OA at 6  $^{\circ}\text{C}$  (2A vs. 6C vs. 6A) and 10  $^{\circ}\text{C}$  (2A vs. 10C vs. 10A) relative to the favourable condition 2C ([Fig. S1A](#)). The data analysis consisted of four major steps: (i) multivariate analyses to (ii) define multivariate interactions between OW and OA, followed by (iii) the identification of biomarkers and (iiib) their functional consequences at the cellular level. This enabled us to (iv) predict shrimp cellular vulnerability under future global change drivers. First (i, [Fig. S1B](#)), we used multivariate analyses to identify, across all measured phospholipids, the general effects of OW and OA across all origins and *per* origin, using Permutational Analysis of Variance (PERMANOVA) and Principal Component Analysis (PCA). We built PERMANOVA models with the terms “origin  $\times$  OW  $\times$  OA” (fixed factors) across all origins and “OW  $\times$  OA” within each origin. When we found at least weak evidence ( $P < 0.1$ ) of non-additive effects using PERMANOVA, we explored the data by subgroups, else we showed the main term effects (*i.e.*, Origin, Temperature or pH). Second (ii, [Fig. S1C](#)), we compared the multivariate thermal responses under current and future pH conditions using the first three PCA dimensions. We also categorised the multivariate interactions between OW and OA as synergisms or antagonisms compared to the null additive model using the first three PCA dimensions rescaled to the reference 2C as delta dimension scores ( $\Delta\text{DS}$ ) ([Fig. S1C](#)). Third (iii, [Fig. S1D](#)), we inferred the functional consequences of exposure to global change drivers. More specifically (iiia), we identified differentially abundant phospholipids (DAP) using the *limma* v3.56.2 R package ([Ritchie et al., 2015](#)). We considered DAP as biomarkers when there was at least “weak evidence”, following FDR adjustment (*i.e.*,  $P_{adj} < 0.1$ ), that their relative abundance levels ( $\text{Log}_2$  Fold-Change, *i.e.*,  $\text{Log}_2\text{-FC}$ ) varied between two experimental conditions. Venn diagrams were used to partition shared and unique DAP between experimental treatments, when comparing the single and combined effects of OW and OA in a 6  $^{\circ}\text{C}$  (2A vs. 6C vs. 6A) and 10  $^{\circ}\text{C}$  (2A vs. 10C vs. 10A) warming scenario, relative to the favourable condition 2C. We classified interactions as synergistic when

phospholipids were most activated in the combined OW + OA treatment but not the single treatments, and as antagonistic when phospholipids were activated by OW but no longer differentially abundant in OW + OA ([Fig. S1D](#)). Next (iiib), we performed functional enrichment analyses to classify phospholipids based on their biophysical, chemical, functional and cellular localisation using the Lipid Ontology (LION) web tool ([Molenaar et al., 2019, 2023](#)) and their unsaturation levels and classes using lipid set enrichment analyses (LSEA) from the *lipidr* v2.14.1 R package ([Mohamed and Molendijk, 2023](#)). When we detected an interaction between OW and OA, we performed a LION qualitative functional enrichment (*i.e.*, using the phospholipid names of the DAP) on either the synergistic or antagonistic partitions of the Venn diagrams. When only a main factor effect of OW or OA was found, a LION quantitative functional enrichment was performed using  $\text{Log}_2$  Fold-Change values of all phospholipids between two experimental conditions of that factor.

To summarise the functional consequences of the synergistic or antagonistic effects of combined OW and OA, we compared between single and combined treatments in moderate vs. severe OW the  $|\text{Log}_2\text{-FC}|$  values of phospholipids associated with the top 10 % (*i.e.*, six of the matched 63 LION terms) of the most enriched LION terms. This was done across and within the top 10 % LION terms. The 63 LION terms associated with phospholipids measured in this experiment are given in [Supplementary Material SM2](#). Last (iv), we summarised the functional analyses into predictions on the cellular vulnerability of shrimp from the four different origins under future combined global change drivers ([Fig. S1E](#)). We used ANOVAs to analyse univariate data ( $|\text{Log}_2\text{-FC}|$ , PCA dimensions and  $\Delta\text{DS}$ ) followed by pairwise *estimated marginal mean* tests from the *emmeans* v1.10.0 R package ([Lenth, 2024](#)) with FDR adjustment for multiple comparisons. Graphs were mainly produced using the *EnhancedVolcano* v1.18.0 ([Blighe, 2018](#)), *ggplot2* v3.4.4 ([Wickham, 2016](#)) and *ggvenn* v0.1.10 ([Yan, 2023](#)) R packages. Multiple letter display was retrieved from the *rcompanion* v2.4.35 R package ([Mangiafico, 2024](#)). Effect sizes (ES) were computed using the *effectsize* v0.8.6 R package ([Ben-Shachar et al., 2020](#)) for PERMANOVA models. ES was expressed with partial Omega-squared ( $p\Omega^2$ ) values as “very small” ( $\text{ES} < 0.02$ ), “small” ( $\text{ES} < 0.13$ ), “medium” ( $\text{ES} < 0.26$ ) and “large” ( $\text{ES} \geq 0.26$ ) ([Cohen, 1992](#)). All raw and processed data and analysis outputs are available on the PANGAEA repository ([Feugere et al., 2025a; 2025b; 2025c](#)) and as Multimedia Components 1-3.

## 3. Results

### 3.1. Phospholipidome responses to OW and OA in shrimp from different origins

We identified 269 phospholipids from nine different classes (see [Table S1](#) for abbreviations and LIPID MAPS common names and lipid classes). The phospholipidome of Northern shrimp from distinct origins responded differently to combined OW and OA, as indicated by strong evidence for a three-way interaction between the terms origin, OW and OA ([Table 1](#)). The effect of origin in isolation contributed the most to defining shrimp phospholipidome profiles ([Table 1](#)), this being visually confirmed through the PCA ([Fig. 1A–B](#)). Shrimp from all four origins differed from each other, and were characterised by unique phospholipidome profiles ([Table 2, Fig. 1B](#)). Notably, shrimp inhabiting the SLE were most different overall from those of all other origins. EC and SLE shrimp displayed the most similar phospholipidome profiles ([Fig. 1B–Table 2](#)). The isolated effect of OW on the phospholipidome profile was most visible between 2 and 10  $^{\circ}\text{C}$ , but was less pronounced when compared to the effect of origin, whilst no overall effect of OA was detected across all origins ([Table 1, Fig. 1CDE](#)).

Given the sheer difference in phospholipidome profiles of shrimp from different origins across the Northwest Atlantic region, we investigated, separately for each geographic origin, the single and combined effects of OW and OA on the shrimp phospholipidome response under warming to either 6 or 10  $^{\circ}\text{C}$  (see [Fig. 2A–D, Table 1](#)).

**Table 1**

Effect of ocean warming (OW) and acidification (OA) and their interaction (OW × OA) on the phospholipidome of the Northern shrimp *Pandalus borealis* across and within four origins in the Northwest Atlantic: St. Lawrence Estuary (SLE), Esquiman Channel (EC), Eastern Scotian Shelf (ESS) and Northeast Newfoundland Coast (NNC). Overall model fits and delta of second-order Akaike Information Criterion ( $\Delta\text{AICc}$ ) relative to null models are given for each model. Terms (origin, OW, OA) and their interactions (×), with at least moderate ( $P \leq 0.05$ ) and weak ( $P \leq 0.1$ , Trend T) evidence are shown in bold and italics, respectively. Df: degrees of freedom. Sum of Sq.: sum of squares.  $R^2$ : variance explained (%). Effect sizes (ES) are given based on partial Omega-squared ( $p\Omega^2$ ) according to Cohen (1992) as “very small” ( $ES < 0.02$ ), “small” ( $ES < 0.13$ ), “medium” ( $ES < 0.26$ ) and “large” ( $ES \geq 0.26$ ). Evidence is given based on Muff et al. (2022), with “little/none” ( $P > 0.1$ ), “weak” ( $P \leq 0.1$ ), “moderate” ( $P \leq 0.05$ ), “strong” ( $P \leq 0.01$ ) and “very strong” ( $P \leq 0.001$ ). Models are adjusted for covariates that have an effect on the lipidome variance: *Batch* of extraction, animal *Mass* and abdominal sample total lipid *Extract*.

Term	Df	Sum of Sq.	$R^2$ (%)	F	P	Evidence	$p\Omega^2$	Effect size
<b>Model 1 – all origins: <math>P = 0.001</math>, <math>R^2 = 47.84</math>, <math>\Delta\text{AICc} = 82.62</math></b>								
Origin	3	15335.8	26	32.23	0.001	Strong	0.3	Large
OW	2	1741.89	3	5.49	0.001	Strong	0.04	Small
OA	1	198.81	0	1.25	0.233	Little/none	0	Very small
OW × OA	2	677.01	1	2.13	0.003	Strong	0.01	Very small
Origin × OW	6	1237.11	2	1.3	0.077 (T)	Weak	0.01	Very small
Origin × OA	3	605.81	1	1.27	0.152	Little/none	0	Very small
Origin × OW × OA	6	1465.72	3	1.54	0.007	Strong	0.01	Very small
Batch	1	5509.29	9	34.73	0.001	Strong	0.13	Medium
Mass	1	680.81	1	4.29	0.001	Strong	0.01	Very small
Extract	1	476.99	1	3.01	0.007	Strong	0.01	Very small
Residual	192	30457.43	52	–	–	–	0.30	–
Total	218	58386.66	100	–	–	–	0.04	–
<b>Model 2 – SLE: <math>P = 0.001</math>, <math>R^2 = 34.96</math>, <math>\Delta\text{AICc} = 9.83</math></b>								
OW	2	676	6	2.09	0.008	Strong	0.04	Small
OA	1	303.28	2	1.87	0.051	Weak	0.02	Very small
OW × OA	2	827.65	7	2.56	0.006	Strong	0.05	Small
Batch	1	2454.12	20	15.17	0.001	Strong	0.20	Medium
Residual	49	7926.59	65	–	–	–	–	–
Total	55	12187.63	100	–	–	–	–	–
<b>Model 3 – EC: <math>P = 0.001</math>, <math>R^2 = 25.72</math>, <math>\Delta\text{AICc} = 0.65</math></b>								
OW	2	699.46	7	2.12	0.007	Strong	0.04	Small
OA	1	188.96	2	1.15	0.277	Little/none	0.00	Very small
OW × OA	2	521.91	5	1.58	0.06 (T)	Weak	0.02	Small
Batch	1	1104.9	11	6.70	0.001	Strong	0.10	Small
Residual	44	7261.24	74	–	–	–	–	–
Total	50	9776.48	100	–	–	–	–	–
<b>Model 4 – ESS: <math>P = 0.001</math>, <math>R^2 = 20.49</math>, <math>\Delta\text{AICc} = 0.87</math></b>								
OW	2	785.2	7	2.25	0.008	Strong	0.04	Small
OA	1	140.69	1	0.81	0.589	Little/none	0.00	Very small
OW × OA	2	431.4	4	1.24	0.19	Little/none	0.01	Very small
Batch	1	932.46	8	5.35	0.001	Strong	0.07	Small
Residual	51	8887.07	80	–	–	–	–	–
Total	57	11176.83	100	–	–	–	–	–
<b>Model 5 – NNC: <math>P = 0.001</math>, <math>R^2 = 37.34</math>, <math>\Delta\text{AICc} = 10.89</math></b>								
OW	2	846.3	9	3.20	0.001	Strong	0.08	Small
OA	1	192.74	2	1.46	0.161	Little/none	0.01	Very small
OW × OA	2	445.80	4	1.69	0.065 (T)	Weak	0.02	Small
Batch	1	2215.88	22	16.77	0.001	Strong	0.23	Medium
Residual	47	6209.19	63	–	–	–	–	–
Total	53	9909.92	100	–	–	–	–	–

The thermal response of shrimp from the three most northerly origins (*i.e.*, SLE, EC and NNC) varied under different seawater pH conditions, as indicated by weak-to-strong evidence for non-additive effects between OW and OA (Table 1). This said, SLE shrimp showed the strongest evidence for interactive effects of combined OW and OA. In contrast, OA did not affect the thermal response of shrimp from the southernmost origin (ESS; Table 1, Fig. 2A–D). Therefore, for shrimp originating from SLE, EC and NNC, we investigated the phospholipidome response to OA combined with OW. Comparing the unique and shared responses to single vs. combined exposure relative to the favourable seawater conditions (*i.e.*, pH 7.75 at 2 °C) evidenced highly origin-dependent synergistic and antagonistic effects of OA and OW (or the absence of an interaction) that changed markedly between 6 and 10 °C (Fig. 3A–E, Table 1, Table S2).

### 3.2. St. Lawrence Estuary (SLE)

Shrimp from the SLE exhibited strong evidence of a non-additive (*i.e.*, an interaction) phospholipidome rewiring when exposed to combined OW and OA, in which the phospholipidome response to temperature depended on seawater pH levels (Table 1, Fig. 2A, 3AB, Fig. S2–4). In effect, exposure to OA conditions caused the emergence of a synergistic phospholipidome response at 6 °C (2C–6C vs. 2C–6A), whilst it triggered an antagonistic effect at 10 °C (2C–10C vs. 2C–10A, Table 2, Fig. 2A, 3AB, Fig. S2–S4). At 6 °C, OA synergistically triggered 43 DAP unique to 2C–6A, involved in key functions such as *plasma membrane*, higher *transition temperature* and *headgroup with a positive charge/zwitter-ion* (Fig. 3A, Fig. S3B). Moreover, superimposing OA on OW at 6 °C synergistically increased and lowered the abundance of sphingomyelins (or

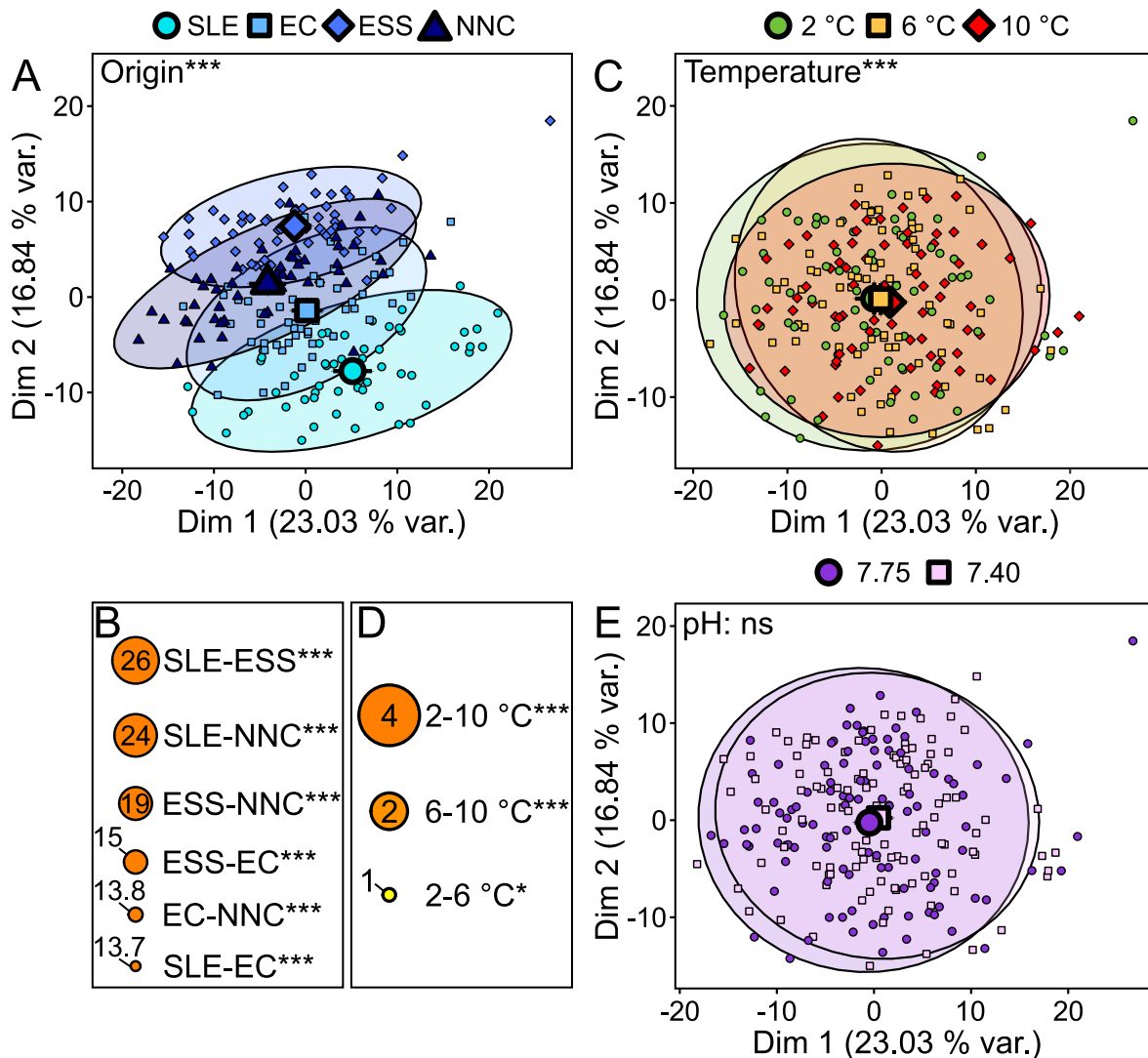


**Fig. 1.** Principal Components Analysis (PCA) showing the effect of (A–B) origin, (C–D) ocean warming (OW) and (E) ocean acidification (OA) on the phospholipidome of the abdominal muscle of females of the Northern shrimp *Pandalus borealis*. Dimensions (Dim) 1 and 2 are shown with their respective variance (var.) contribution to phospholipidome profiles of shrimp across the Northwest Atlantic, from the St. Lawrence Estuary (SLE), Esquiman Channel (EC), Northeast Newfoundland Coast (NNC) and Eastern Scotian Shelf (ESS). In (C), temperature treatments (in °C) are 2 (green circles), 6 (orange squares) and 10 (red diamonds). In (E), OA (pH 7.40) is represented by lilac coloured squares when compared to control seawater pH (7.75, purple circle). Pairwise comparisons of origin (B) and OW (D) are shown with circles of different sizes and values representing the explained var. percentages ( $100 \times R^2$ ) ordered by largest to smallest differences from top to bottom. Asterisks represent statistical evidence for the effects of origin, OW, OA and group comparisons with  $P < 0.05^*$  and  $P < 0.001^{***}$ . ns: no evidence of an effect. Small shapes represent individual data points ( $n = 219$ ). Centroids are represented by large shapes with error bars depicting their 95 % confidence intervals (CI) along Dim 1 and Dim 2 and ellipses show 95 % CI of multivariate t-distributions. (For interpretation of the references to colour in this figure legend, the reader is referred to the Web version of this article.)

phosphosphingolipids, SM) and cardiolipins (or glycerophosphoglycerophosphoglycerols, CL), respectively (Fig. S3E) and favoured the accumulation of less unsaturated phospholipids whilst decreasing highly unsaturated phospholipids (Fig. S2F). On the other hand, exposure to OA conditions had an antagonistic effect on the phospholipidome that limited the temperature-driven decrease in phosphatidylglycerols (or glycerophosphoglycerols, PG) and increase in phospholipids and phosphatidylcholines (or glycerophosphocholines, PC), associated with *neutral intrinsic curvature, low transition temperature, above average lateral diffusion, below average bilayer thickness* (2C–10C vs. 2C–10A, Fig. 3B, Fig. S3, S3C–F). Whilst SLE shrimp showed little phospholipidome plasticity as they did not display the expected lowering in highly unsaturated phospholipids in response to the exposure to 10 °C alone (slope  $P = 0.32$ ), they still increased the abundance of phospholipids with a lower degree of unsaturation ( $n = 2$ ). However, this response was

no longer present at pH 7.40, once again evidencing the antagonistic phospholipidome response to OA combined with 10 °C in SLE shrimp (Fig. S3F). Consequently, the thermal gradient response of SLE shrimp was non-additive, shifting from synergistic to antagonistic under OA conditions between 6 and 10 °C, respectively (Fig. S4). Notably, whilst the overall synergistic patterns at 6 °C and antagonistic at 10 °C were visualised on the first two dimensions of the PCA (totalling c. a. 42 % explained variance), there were indications of antagonism in dimension 3 (8.92 % explained variance), suggesting that at least a minor fraction of the phospholipids responded in an opposite manner to the combined exposure to OW and OA in SLE shrimp (Fig. S4). In addition, SLE shrimp were responsive to the isolated effects of OW, albeit this effect was small, whilst there was weak evidence for an overall very small effect of OA (Table 1).

**Table 2**

**Pairwise comparisons of origin, OW and OA groups for the phospholipidome response of the Northern shrimp.** Based on PERMANOVA results, pairwise comparisons are given for OW across all origins and for Eastern Scotian Shelf (ESS), whilst pairwise comparisons of single and combined conditions of OW and OA are given relative to the favourable condition 2C for St. Lawrence Estuary (SLE), Esquiman Channel (EC) and Northeast Newfoundland Coast (NNC). Effects of treatments with at least moderate ( $P \leq 0.05$ ) and weak ( $P \leq 0.1$ , Trend T) effects are shown in bold and italics, respectively.  $R^2$ : variance explained (%). Sum of Sq.: sum of squares. Effect sizes (ES) are given based on partial Omega-squared ( $p\Omega^2$ ) according to Cohen (1992) as “very small” ( $ES < 0.02$ ), “small” ( $ES < 0.13$ ), “medium” ( $ES < 0.26$ ) and “large” ( $ES \geq 0.26$ ). Evidence is given based on Muff et al. (2022), with “little/none” ( $P > 0.1$ ), “weak” ( $P \leq 0.1$ ), “moderate” ( $P \leq 0.05$ ), “strong” ( $P \leq 0.01$ ) and “very strong” ( $P \leq 0.001$ ). Models are adjusted for covariate effects.  $P_{adj}$  are False Discovery Rate adjusted p-values for multiple testing.

Group 1	Group 2	Sum of Sq.	$R^2$ (%)	F	$P_{adj}$	Evidence	$p\Omega^2$	Effect size
<b>All origins</b>								
SLE	ESS	8311.73	26	47.63	0.0001	Very strong	0.29	Large
SLE	NNC	6827.73	24	44.73	0.0001	Very strong	0.28	Large
ESS	NNC	4823.22	19	30.35	0.0001	Very strong	0.21	Medium
ESS	EC	3803.45	15	22.19	0.0001	Very strong	0.16	Medium
EC	NNC	3167.00	14	20.78	0.0001	Very strong	0.16	Medium
SLE	EC	3482.63	14	20.78	0.0001	Very strong	0.16	Medium
2 °C	6 °C	410.89	1	2.48	0.0111	Moderate	0.01	Very small
2 °C	10 °C	1486.04	4	8.89	0.0003	Very strong	0.05	Small
6 °C	10 °C	653.83	2	4.07	0.0003	Very strong	0.02	Small
<b>SLE</b>								
2C	2A	407.62	9	2.38	0.0726 (T)	Weak	0.07	Small
2C	6C	149.45	4	0.97	0.4142	Little/none	0.00	Very small
2C	6A	582.75	14	3.39	0.0180	Moderate	0.12	Small
2C	10C	575.06	14	3.54	0.0180	Moderate	0.13	Small
2C	10A	280.51	7	1.62	0.1512	Little/None	0.04	Small
6A	10A	288.37	8	1.66	0.1350	Little/None	0.04	Small
<b>EC</b>								
2C	2A	204.25	7	1.35	0.2126	Little/none	0.02	Small
2C	6C	308.82	11	1.89	0.1010	Little/none	0.05	Small
2C	6A	187.26	7	1.29	0.2126	Little/none	0.02	Very small
2C	10C	338.07	8	1.8	0.1377	Little/none	0.04	Small
2C	10A	470.33	16	3.44	0.0048	Strong	0.12	Small
6A	10A	336.71	14	2.47	0.0093	Strong	0.08	Small
<b>NNC</b>								
2C	2A	497.96	19	3.8	0.0052	Strong	0.15	Medium
2C	6C	301.66	14	2.58	0.0265	Moderate	0.10	Small
2C	6A	373.82	15	2.68	0.0347	Moderate	0.11	Small
2C	10C	738.99	25	5.78	0.0052	Strong	0.25	Medium
2C	10A	536.43	20	3.63	0.0052	Strong	0.17	Medium
6A	10A	189.58	5	1.27	0.2275	Little/None	0.01	Very small
<b>ESS</b>								
2 °C	6 °C	214.21	3	1.11	0.2969	Little/none	0.00	Very small
2 °C	10 °C	606.32	8	3.47	0.0027	Strong	0.06	Small
6 °C	10 °C	356.35	5	2.24	0.0237	Moderate	0.03	Small

### 3.3. Esquiman Channel (EC)

Shrimp from the EC showed weak evidence for a small non-additive effect of combined OW and OA (Table 1). Particularly, EC shrimp displayed an antagonistic response at 6 °C that became synergistic at 10 °C (Fig. 2, Fig. S5-7). Indeed, at 6 °C and pH 7.75, EC shrimp altered the abundance of five DAP [i.e., 2C-6C; PC(32:0), PC(36:1), PC(38:0), PI (38:4) and PE(42:8)] involved in higher bilayer thickness and transition temperature but lower lateral diffusion, that drastically decreased and were no longer differentially abundant at pH 7.40 (2C-6A, Fig. 3D, Fig. S5-7). This antagonistic effect was also evident as OA limited the OW-driven greater abundance of phosphatidylserines (or glycerophosphoserines, PS) and SM and lower abundance of PC (Fig. S6A,B,E). In contrast, exposure to 10 °C alone only activated a response of five DAP [i.e., PC(O-30:0), PC(34:4), PC(32:1), PE(38:3) and PC(O-37:1)/PC (P-37:0)], whilst it triggered the accumulation of another 22 unique DAP when superimposed with OA (2C-10A, Fig. 3E, Fig. S5-7). This synergistic effect at 10 °C was associated with an overall increase in PS and

decrease in PC, particularly associated with key functions such as plasma membrane, high lateral diffusion, very low transition temperature, headgroup with negative charge and low bilayer thickness (Fig. S6C-F). The interaction between OW and OA caused the thermal response to differ under current and low seawater pH in EC shrimp, although this varied depending on the dimension investigated (Fig. S7). However, EC shrimp were able to adjust their membrane fluidity in response to both 6 and 10 °C, regardless of seawater pH (Fig. S6F). Finally, EC shrimp were impacted by the isolated small effect of OW but not by OA alone (Table 1, Fig. S5).

### 3.4. Northeast Newfoundland Coast (NNC)

There was weak evidence of an interaction between OW and OA on the phospholipidome of NNC shrimp (Table 1, Fig. 2C, Fig. S8-S10). All scenarios of OW and OA in isolation and combined altered phospholipidome profiles compared to the favourable condition 2C (Table 2). However, in terms of biomarkers, these responses were somewhat

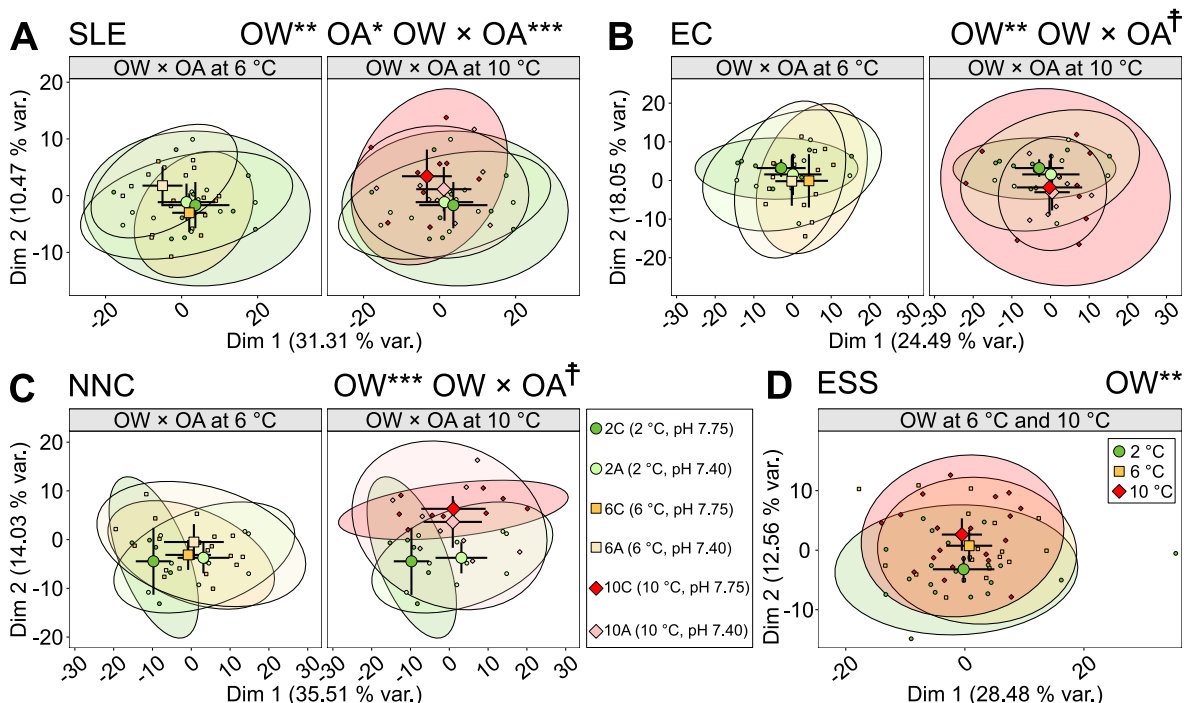


**Fig. 2.** PCA showing the effect of OW and OA on the phospholipidome of the abdominal muscle of females of the Northern shrimp. Data is shown for shrimp from the (A) SLE, (B) EC, (C) NNC and (D) ESS. Temperature treatments (in °C) are 2 (green circle), 6 (orange square) and 10 (red diamond). pH treatments are control (pH 7.75, “C” suffix) and OA (faint coloured shapes, pH 7.40, “A” suffix). Due to evidence of non-additive effects of OW and OA, data for SLE, EC and NNC show the single vs. combined effects of OA at 6 °C (i.e., 2C vs. 2A, 6C and 6A, left split panels) and 10 °C (i.e., 2C vs. 2A, 10C and 10A, right split panels). For ESS, only the effect of OW is shown. Small shapes represent individual data points. Centroids are represented by large shapes with error bars depicting their 95 % CI along dimensions (Dim) 1 and 2. Ellipses show 95 % CI of multivariate t-distributions. The effects of OW, OA and their interaction are shown in the top-left corners when  $P \leq 0.1$  (weak evidence shown with †),  $P \leq 0.05^*$ ,  $P \leq 0.01^{**}$ ,  $P \leq 0.001^{***}$  and  $P \leq 0.0001^{****}$ . (For interpretation of the references to colour in this figure legend, the reader is referred to the Web version of this article.)

limited since there were no DAP in NNC shrimp experiencing warming to 6 °C (2C–6C) or lowered pH (2C–2A), even in combination (2C–6A, Fig. S8). However, there was an indication for the presence of a synergistic response concerning the enhanced abundance in SM and PC and the lowered abundance in phosphatidylethanolamines (or glycerophosphoethanolamines, PE) and PG (Fig. S9C). This synergistic effect was accompanied by the deviation of phospholipid unsaturation profiles, with a negative relationship between unsaturation levels and phospholipid abundance only appearing when NNC shrimp were exposed to 6 °C at low pH (Fig. S9D). In contrast, an antagonistic response of combined OA and OW to 10 °C was evidenced by the loss of the expected response to warming under current vs. OA conditions (2C–10C vs. 2C–10A; Fig. S8–S9). The most enriched temperature-driven functions that were no longer differentially abundant under OW combined with OA were involved in higher *bilayer thickness* and *transition temperature* and lower *lateral diffusion*. The change in their associated DAP tended to confirm this antagonistic pattern (Fig. 3C, Fig. S9A–B). Likewise, OA slightly dampened the increase in PS in response to 10 °C (Fig. S9C). The combined effects of OW and OA led NNC shrimp to display different phospholipidome profiles in response to the thermal gradient in current and lowered seawater pH conditions, although this again varied with the principal component dimension (Fig. S10). However, the antagonistic effect of OA did not prevent shrimp from maintaining overabundant less unsaturated phospholipids in response to warming, as Pearson’s correlation coefficients and  $P$  of slopes remained similar (2C–10C vs. 2C–10A, Fig. S9D). Last, the phospholipidome profiles of NNC shrimp were impacted by the isolated small effect of OW but not by that of OA alone (Table 1).

### 3.5. Eastern Scotian Shelf (ESS)

There was strong evidence that only OW had a small effect on the phospholipidome of ESS shrimp, which was only present at 10 °C (Tables 1–2, Fig. 2D, Fig. S11A–D). Compared to 2 °C, ESS shrimp overall displayed lower abundance of *glycerophospholipids*, notably of PC, but increased SM abundance at 10 °C. The DAP were involved in higher *transition temperature* and *bilayer thickness* but lower *lateral diffusion* and *endoplasmic reticulum* (Fig. 3F, Fig. S12A). In addition, exposure to 6 °C and most particularly to 10 °C triggered a more pronounced increase in the levels of less unsaturated phospholipids accompanied by a simultaneous decrease in highly unsaturated ones (Fig. S12B). No effect of OA was found, neither alone nor in combination with OW (Table 1).

### 3.6. Shifts from moderate to severe OW combined with OA

Origin-specific interactions suggested shifts from synergisms to antagonisms (and vice versa) in thermal responses depending on pH in SLE, NNC and EC shrimp. To explore this further, we directly compared the phospholipidome profiles of shrimp exposed to OA combined with moderate vs. severe OW (6A–10A). Whilst there were pronounced differences in the overall phospholipidome profiles of EC shrimp, subtler changes in classes and unsaturation profiles were observed for SLE and NNC shrimp, when they experienced OA combined with more severe OW, compared to the more moderate OW scenario (Table S2, Fig. S13).

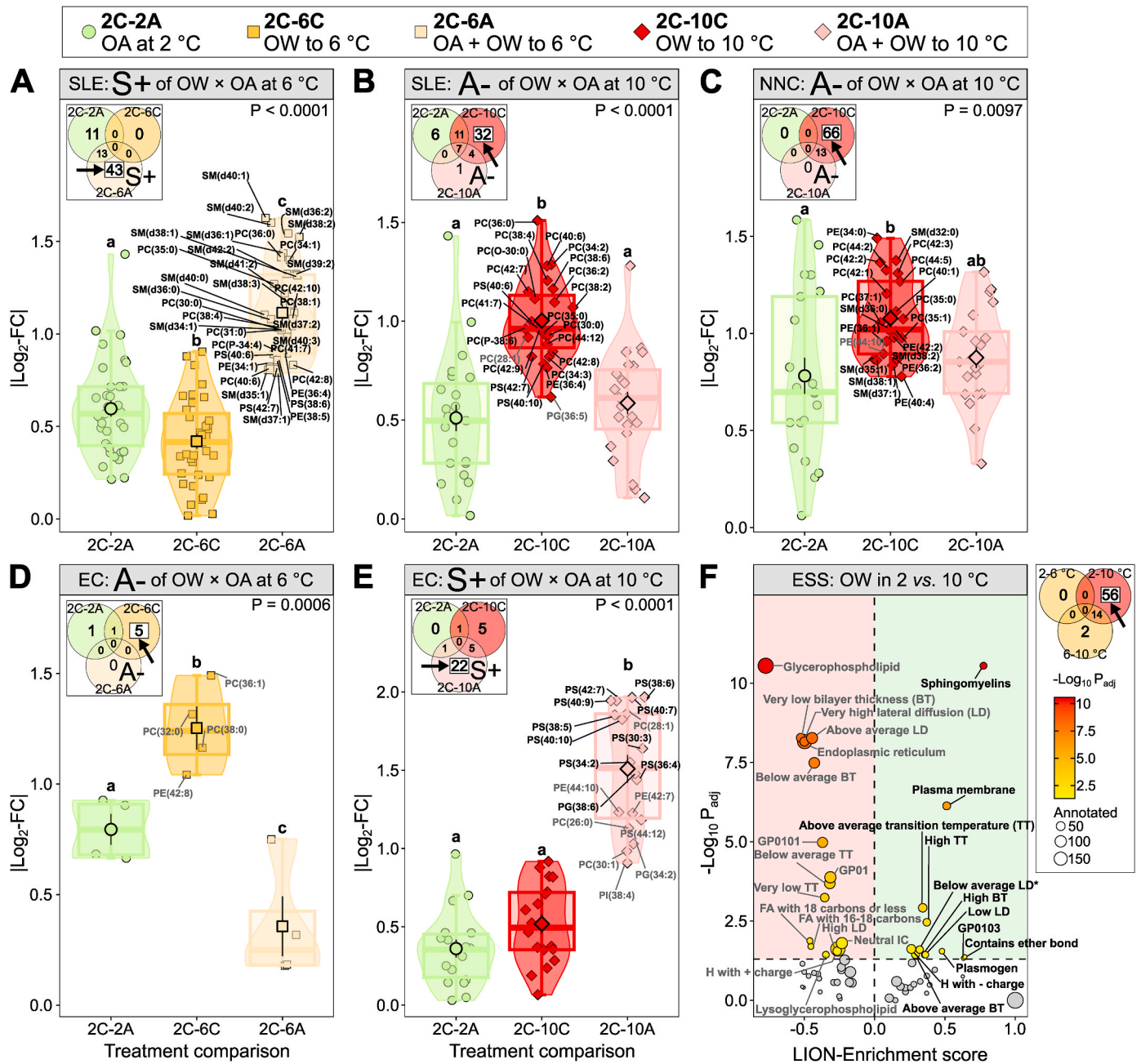


**Fig. 3. Functional phospholipidome analysis of the effects of OW and OA on the abdominal muscle of females of the Northern shrimp.** Data is shown for the (A–B) SLE, (C) NNC, (D–E) EC and (F) ESS. For origins (SLE, EC and NNC) with at least weak evidence ( $P < 0.1$ ) for an interaction effect of OW and OA, data represent, for each contrast group relative to the favourable condition 2C, the change in phospholipid abundance in the single and combined exposure to OA and OW at either 6 or 10 °C: 2C-2A, 2C-6C, 2C-6A, 2C-10C, 2C-10A. For NNC, changes were only observed at 10 °C. Data in (A–E) shows the  $|\text{Log}_2\text{-FC}|$  (absolute  $\text{Log}_2$  Fold-Change, increasing and decreasing in black and grey, respectively) per treatment of phospholipids considered differentially abundant (DAP) in the Venn diagram partitions indicated by arrows. Venn Diagrams indicate synergisms ( $S^+$ , i.e., DAP only found in combined treatments 6A or 10A) or antagonisms ( $A^-$ , i.e., DAP only altered by OW alone in 6C or 10C, but not when combined with OA in 6A and 10A). Synergism is observed if the  $|\text{Log}_2\text{-FC}|$  values are higher than single factor effects. Antagonism is observed if  $|\text{Log}_2\text{-FC}|$  values are lower in OA + OW than in OW. Individual points in (A–E) are  $|\text{Log}_2\text{-FC}|$  values of individual phospholipids associated with the top 10 % most enriched Lipid Ontology (LION) terms of the indicated Venn diagram partition. Large shapes are mean values  $\pm$  95 % CI.  $P$ -values on top-right corners represent the level of statistical evidence of treatment effect relative to 2C. Different lowercase letters above the violin plots indicate differences in abundance between contrast groups. For ESS (F, independent legend to its right), no interactive effects of OW and OA were observed and data represent only the temperature effect in 2 vs. 10 °C. In (F), the functional analysis shows the statistical evidence level ( $-\text{Log}_{10} P_{\text{adj}}$ , y-axis) as a function of LION-Enrichment score (x-axis) with circle sizes indicating the number of annotated phospholipids per LION term. Individual dots represent LION terms, with labels when  $P_{\text{adj}} < 0.05$  (above horizontal dashed line), with average overabundance (black font, green area) or underabundance (grey font, red area) of their associated phospholipids at 10 °C relative to 2 °C. FA: fatty acid; GP01: glycerophosphocholines; GP0101: diacylglycerophosphocholines; GP0103: 1-(1z-alkenyl),2-acylglycerophosphocholines; IC: intrinsic curvature. See [Supplementary Material SM3](#) for corresponding data tables. (For interpretation of the references to colour in this figure legend, the reader is referred to the Web version of this article.)

4. Discussion

We report for the first time the presence of complex origin-dependent non-additive responses to combined OW and OA within the phospholipidome of an ecologically and economically important marine invertebrate. Further, we evidence origin-specific physiological shifts (*i.e.*, from synergistic to antagonistic and *vice versa*) from moderate (6 °C) to severe (10 °C) OW combined with OA. Our results corroborate the existence of a high level of intraspecific variation in marine ectotherms' molecular responses, showcasing the importance of accounting for such variation when predicting species' vulnerability in future oceans.

4.1. Origin-specific shifts of the shrimp phospholipidome under combined OW and OA

Northern shrimp from each origin in the Northwest Atlantic display highly distinctive phospholipidome profiles, corroborating their metabolomics (Guscelli et al., 2023a), transcriptomics (Leung et al., 2023) and genetic (Bourret et al., 2024) differences. The reported genetic differentiation may partly explain the observed inter-origin divergence in the response to combined OW and OA. Whilst shrimp from the three most northern origins (*i.e.*, SLE, EC and NCC) are sensitive to combined OW and OA, those from the southernmost origin (*i.e.*, ESS) seem only sensitive to severe OW. Relative to EC and NNC shrimp, SLE shrimp are the most sensitive to the combined effects of OW and OA at the phospholipidome level, mirroring the sensitivity of their metabolome (Guscelli et al., 2023a). Given the ongoing sharp regional declines in shrimp populations and concurrent environmental changes in the Northwest Atlantic (Bourdages et al., 2022), we expected shrimp to display synergistic responses under combined OW and OA. Instead, shrimp show complex origin- and scenario-dependent non-additive responses (both synergistic and antagonistic), suggesting different physiological responses will likely be at play in different shrimp populations and stocks under future global change scenarios (Fig. 4).

The functional enrichment helps predict the physiological outcome of exposure to combined OW and OA. Particularly, a lower membrane

fluidity and stability can be expected when more unsaturated phospholipids, which are associated with lower (membrane phase) transition temperature and higher lateral diffusion, and a lower bilayer thickness are observed (Molenaar et al., 2019; Wassenaar et al., 2015). Given that we hypothesised shrimp to counteract, *via* homeoviscous adaptation, the higher fluidity and thinner membranes driven by elevated temperatures (Dymond, 2015; Kučerka et al., 2011; Sinensky, 1974), we interpret these negative physical properties of the membrane as a sign of higher cellular vulnerability. With this in mind, we use the phospholipidome functional enrichment to predict the cellular membrane physiological status of shrimp from each origin in the Northwest Atlantic when OA is combined with moderate or severe OW (Fig. 4).

Overall, shrimp across the studied area seem tolerant to moderate OW alone. However, when moderate OW is combined with OA, it alters the membrane profiles of shrimp inhabiting SLE, EC and NNC, but not ESS. Specimens from both NNC and SLE display synergistic patterns when OA is superimposed on moderate OW. This synergistic rewiring of the phospholipidome involves higher accumulation of SM and less unsaturated phospholipids, possibly to allow cell membrane viscosity acclimation (El Babili et al., 1997; Sinensky, 1974). Specimens from the SLE additionally show overabundant phospholipids involved in *high transition temperature*. Overall, this membrane remodelling suggests that both SLE and NNC shrimp are able to maintain their membrane homeostasis under OA combined with moderate OW (Dymond, 2015; Hazel, 1995; Sinensky, 1974) (Fig. 4). Contrasting with SLE and NNC shrimp, specimens from the EC show an antagonistic pattern, which causes them to lose their capacity to thermally acclimate their cell membranes when OA is superimposed on moderate OW (Fig. 4). Such acclimation capacity to OW and OA was likewise reported in gastropods (Lischka et al., 2022), and in an eurytherm polar cod but not in its stenothermal counterpart (Leo et al., 2020). This suggests ESS, SLE and NNC shrimp are more thermally competent than their EC counterparts.

A key finding from our study is the physiological shift from synergisms to antagonisms, or *vice versa*, when shrimp experience OA combined with severe OW, as they are closer to their thermal limits (Baker et al., 2024; Chemel et al., 2020; Shumway, 1985, Fig. 4). Given that

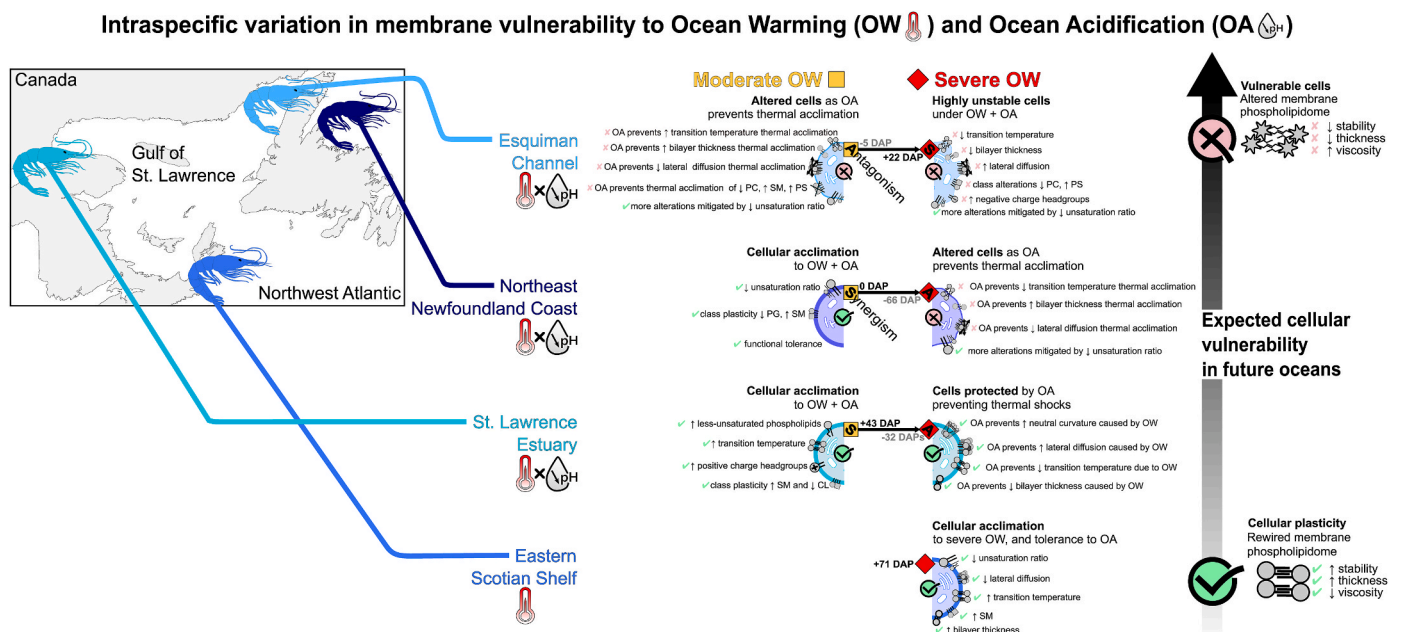


Fig. 4. Intraspecific variation in the sensitivity of the phospholipidome of the abdominal muscle of females of the Northern shrimp under combined OW and OA. Shrimp phospholipidome profiles show differential functional consequences and shifts in the mode of physiological responses when OA is combined with more severe OW compared to more moderate OW. Functions are associated with differentially abundant phospholipids (DAP, indicated by numbers) that change with OW alone or with OA (+n DAP), or that no longer show thermal responses when OA is present (-n DAP). CL: Cardiolipin, PC: Phosphatidylcholine, PG: Phosphatidylglycerol, PS: Phosphatidylserine, SM: Sphingomyelin.

shrimp from the same experiment show higher mortality beyond 6 °C (Guscelli et al., 2023b), we can expect the phospholipidome rewiring to play a key role either in underlying risks of mortality, or if there is a survivor bias, in enabling shrimp to survive these stressful conditions. In the future ocean scenario, SLE and NNC shrimp display antagonistic phospholipidome responses, though opposite mechanisms are involved. Indeed, compared to shrimp from other populations, SLE shrimp exposed to severe OW alone appear less capable to compensate for the expected temperature-driven increase in membrane fluidity, according to the acclimatory homeoviscous adaptation theory (Malekar et al., 2018). Contrastingly, shrimp from NNC seem able to maintain stable membranes under elevated temperatures by increasing the abundance of SM, less unsaturated phospholipids and phospholipids involved in higher *transition temperature* and *bilayer thickness*, whilst lowering low *lateral diffusion*-associated phospholipids' abundance. Altogether, such patterns may protect cells against higher temperatures by maintaining constant viscosity to guarantee membrane stability (Mužić et al., 2019; Patton et al., 1992; Sinensky, 1974). Consequently, the antagonistic effect of OA on severe OW prevents thermal acclimation in NNC shrimp, whilst buffering the adverse impacts of thermal shock in SLE shrimp (Fig. 4). Contrastingly, in EC shrimp, OA combined with severe OW synergistically drives higher *lateral diffusion*, lower *transition temperature* and decreases *bilayer thickness*, likely indicating membrane instability (Molenaar et al., 2019). Whilst the overall effect of OA is weak in our study, we report that it can still alter the thermal response of marine metazoans. In line with this, recent meta-analyses reported that combined OW and OA triggers overall antagonistic effects at the whole-organism level in marine invertebrates (Alter et al., 2024). In contrast, lipidomic responses tend towards synergism in Arctic pteropods (Lischka et al., 2022). The divergent molecular-level interactive effects of OW and OA we observe here confirm that more complex mechanisms occur in lower biological organisation compartments (Madeira et al., 2017), including in the Northern shrimp (Guscelli et al., 2023a, 2023b). Of note, the phospholipidome also shows subtle differences when directly comparing shrimp's profiles under OA combined with moderate vs. severe OW, confirming that different non-additive patterns emerge when OA is superimposed on more severe OW.

#### 4.2. Integrated assessment of origin-specific vulnerability to combined OW and OA

Most importantly, we report intraspecific variation in the phospholipidome plasticity and sensitivity to combined OW and OA. Integrating the newly acquired understanding of the phospholipidome response to OW and OA (this study), with observations of their cellular energy capacity, metabolome, whole-organism physiology and survival on the same shrimp specimens (Guscelli et al., 2023a, 2023b) and the characterisation of their natural environments, we can infer which populations are most at risk under future climate changes (Fig. 4). Strikingly, shrimp from different origins showed, overall, highly comparable whole-organism performances under combined severe OW and OA scenarios, in terms of survival, metabolic rates and aerobic capacity (Guscelli et al., 2023b). However, they showed different intraspecific cellular sensitivity to combined severe OW and OA both within the metabolome (Guscelli et al., 2023a) and phospholipidome (this study). These findings confirm that the molecular responses of marine species to environmental stressors appear most sensitive compared to their whole-organism physiology (Madeira et al., 2024; Noisette et al., 2021; Smit et al., 2009). Particularly, compared to shrimp from ESS, specimens inhabiting the SLE, EC and NNC appear most sensitive to combined OW and OA. Our study supports previous reports of interregional molecular variation in the response to global change drivers (Calosi et al., 2017; Schmidt and Donelson, 2024; Thor et al., 2018). Such phenotypic plasticity could enable different populations to persist under a changing ocean (Calosi et al., 2016; Foo and Byrne, 2016). Our findings highlight the role of the cell membrane phospholipidome, a major yet largely

understudied functional cellular compartment (Kyle et al., 2021; Swinnen and Dehairs, 2022), as a powerful biomonitoring tool of animal health in response to environmental stressors (Dreier et al., 2020; Tang et al., 2019). For instance, the shrimp from SLE we used in this study are the most sensitive ones to combined OW and OA at the metabolome level (Guscelli et al., 2023a). These SLE shrimp also show the most pronounced response to combined OW and OA, which may be a compensation mechanism allowing their cellular membranes to remain stable despite these stressful scenarios (Fig. 4). Similar to other marine ectotherms (Käkelä et al., 2008; Winnikoff et al., 2024), this suggests the presence for membrane adaptation and/or long-term acclimatisation to prevalent local environmental regimes. This corroborates their possible local adaptation/acclimatisation at the cellular energetic and metabolomic levels (Guscelli et al., 2023a, 2023b). However, this molecular sensitivity at the lipidome and metabolome level under combined OW and OA may incur costs to SLE shrimp, as they show the poorest whole-organism physiological condition (Guscelli et al., 2023b). In contrast, whilst EC and NNC shrimp do not show shifts of energy metabolome in response to OA either alone or with OW (Guscelli et al., 2023b), their cellular membrane integrity appears most negatively impacted by combined OW and OA (Fig. 4). For instance, EC shrimp show lower bilayer thickness and higher lateral diffusion suggesting their membranes are overly fluid and highly permeable, at risk of proton leak and unstable membrane-bound enzyme activities (Frallicciardi et al., 2022; Leo et al., 2020). In turn, such adverse membrane patterns may compromise the general biological functioning of EC shrimp (Hazel, 1990). Organisms living near their upper thermal limits may, in fact, be most at risk under global changes due to their limited homeoviscous adaptation capacity (Muir et al., 2016). In this sense, our findings suggest that shrimp from the Esquiman Channel (*i.e.*, EC) already operate at their upper stress tolerance limit due to ongoing OW and OA (Bourdages et al., 2022; Mucci et al., 2018) compared to less prominent OA in ESS waters (DFO, 2022a, 2020). As opposed to SLE shrimp, those from EC may not have moved bathymetrically to seek more favourable conditions (Bourdages et al., 2022). Altogether, the phospholipidome, metabolome and whole-body physiology data combined with their *in-situ* monitoring suggest that EC shrimp are most at risk of cellular failure in future oceans (Guscelli, 2024; Guscelli et al., 2023a, 2023b). Therefore, we suggest they should be a priority target for conservation strategies among the populations tested here (Fig. 4).

In conclusion, we show a high degree of intraspecific variation in a marine ectotherm's cellular membrane vulnerability to combined global changes, with important implications for ecosystems' stability and resilience (Mimura et al., 2017; Vázquez et al., 2023). Furthermore, our results on phospholipidome, when combined with insights from prior works on whole-body (Guscelli et al., 2023b), and metabolome (Guscelli et al., 2023a) responses of the same specimens, reveal compartment- and origin-specific sensitivities to combined global changes. This highlights the importance of considering multiple levels of the biological hierarchy using a macrophysiological approach (Bozinovic et al., 2011; Chown and Gaston, 2008; Gaston et al., 2009) to refine predictions on the fate of biotic systems in the context of global changes. Moreover, functionally characterising the presence of non-additive responses to multiple global change drivers is paramount to predicting biological systems' emerging properties and supporting their effective management (Carrier-Belleau et al., 2021; Côté et al., 2016; Piggott et al., 2015). Altogether, our findings highlight that OA alters in complex ways ectotherms' molecular responses to OW, suggesting large uncertainties on the consequences of combined global change drivers on biological systems, calling for the development of highly integrative approaches (Madeira et al., 2024).

#### CRedit authorship contribution statement

**Lauric Feugere:** Writing – review & editing, Writing – original draft, Visualization, Validation, Methodology, Investigation, Formal analysis, Data curation, Conceptualization. **Joana Filipa Fernandes:** Writing –

review & editing, Visualization, Validation, Methodology, Investigation, Formal analysis, Data curation, Conceptualization. **Ella Guscelli:** Writing – review & editing, Visualization, Validation, Methodology, Investigation, Data curation, Conceptualization. **Tânia Melo:** Writing – review & editing, Methodology, Investigation. **Susana Aveiro:** Writing – review & editing, Methodology, Investigation. **Denis Chabot:** Writing – review & editing, Supervision, Resources, Methodology, Conceptualization. **Ricardo Calado:** Writing – review & editing, Validation, Supervision, Resources, Methodology, Conceptualization. **Rosário Domingues:** Writing – review & editing, Validation, Supervision, Resources, Methodology, Funding acquisition, Conceptualization. **Diana Madeira:** Writing – review & editing, Validation, Supervision, Resources, Project administration, Methodology, Funding acquisition, Conceptualization. **Piero Calosi:** Writing – review & editing, Visualization, Validation, Supervision, Resources, Project administration, Methodology, Funding acquisition, Conceptualization.

### Ethical statement

All experiments were conducted in agreement with the Canadian legislation for animal experimentation since the Canadian Council for Animal Care does not require ethics approval for experimentation with crustaceans.

### Funding

This work was supported by (1) a MITACS Accelerate grant [IT35557 to PC], (2) an OURANOS grant [554023 to DC and PC], (3) a Department of Fisheries and Oceans Canada Strategic Program for Ecosystem Based Research and Advice grant and an Aquatic Climate Change Adaptation Services Program grant to DC, (4) a MITACS-Ouranos Accelerate grant, a Fonds institutionnel de recherche (FIR) de l'Université du Québec a Rimouski (UQAR) grant, a Canada Foundation for Innovation grant (36665) and Natural Sciences and Engineering Research Council of Canada (NSERC) Discovery Grants [RGPIN-2015-06500 and RGPIN-2020-05627] to PC, (5) a Fonds de Recherche du Québec - Nature et Technologies (FRQNT) scholarship (PBEEE, 289597) and a Réal-Decoste Ouranos scholarship (286109) to EG, (6) a Fundação para a Ciência e a Tecnologia (FCT) PhD Scholarship [2021.04675.BD to JFF] and (7) Scientific Employment Stimulus researcher contract granted to DM (CEECIND/01250/2018) and (8) the financial support to CESAM (UIDP/50017/2020+UIDB/50017/2020+LA/P/0094/2020) to RC, RD and DM. LF acknowledges support by a MITACS Accelerated grant [IT35557].

### Declaration of competing interest

The authors declare that they have no known competing financial interests or personal relationships that could have appeared to influence the work reported in this paper.

### Acknowledgements

This work was supported by (1) a MITACS Accelerate grant [IT35557 to PC], (2) an OURANOS grant [554023 to DC and PC], (3) a Department of Fisheries and Oceans Canada Strategic Program for Ecosystem Based Research and Advice grant and an Aquatic Climate Change Adaptation Services Program grant to DC, (4) a MITACS-Ouranos Accelerate grant, a Fonds institutionnel de recherche (FIR) de l'Université du Québec à Rimouski (UQAR) grant, a Canada Foundation for Innovation grant (36665) and Natural Sciences and Engineering Research Council of Canada (NSERC) Discovery Grants [RGPIN-2015-06500 and RGPIN-2020-05627] to PC, (5) a Fonds de Recherche du Québec - Nature et Technologies (FRQNT) scholarship (PBEEE, 289597) and a Réal-Decoste Ouranos scholarship (286109) to EG, (6) a Fundação para a Ciência e a Tecnologia (FCT) PhD Scholarship [2021.04675.BD to JFF] and (7) a

Scientific Employment Stimulus researcher contract granted to DM (2022.00153.CEECIND, <https://doi.org/10.54499/2022.00153.CEECIND/CP1720/CT0016>) and (8) the financial support to CESAM (UIDP/50006 + LA/P/0094/2020) to RC, RD and DM. LF acknowledges support by a MITACS Accelerated grant [IT35557].

### Appendix A. Supplementary data

Supplementary data to this article can be found online at <https://doi.org/10.1016/j.envres.2025.122135>.

### Data availability

All data is available on the PANGAEA® Data Publisher. All processed data are given as Supplementary Material in [Multimedia Components 1, 2, 3](#). All R code is available as Supplementary Material in [Multimedia Components 4 and 5](#). Supplementary Methods, Supplementary Figures and Supplementary Tables are available as a Supplementary Information file ([Multimedia Component 6](#)).

### References

- Alter, K., Jacquemont, J., Claudet, J., Lattuca, M.E., Barrantes, M.E., Marras, S., Manríquez, P.H., González, C.P., Fernández, D.A., Peck, M.A., Cattano, C., Milazzo, M., Mark, F.C., Domenici, P., 2024. Hidden impacts of ocean warming and acidification on biological responses of marine animals revealed through meta-analysis. *Nat. Commun.* 15, 2885. <https://doi.org/10.1038/s41467-024-47064-3>.
- Baker, K., Mullaney, D., Fulton, S., 2024. Spatiotemporal modelling of northern shrimp *Pandalus borealis* distribution patterns throughout Canada's subarctic and arctic regions. *Mar. Ecol. Prog. Ser.* 740, 79–93. <https://doi.org/10.3354/meps14651>.
- Bartholomew, G.A., 1986. The role of natural history in contemporary biology. *Bioscience* 36, 324–329. <https://doi.org/10.2307/1310237>.
- Ben-Shachar, M.S., Lüdtke, D., Makowski, D., 2020. Effectsize: estimation of effect size indices and standardized parameters. *J. Open Source Softw.* 5, 2815. <https://doi.org/10.21105/joss.02815>.
- Bergé, J.-P., Barnathan, G., 2005. Fatty acids from lipids of marine organisms: molecular biodiversity, rolessas biomarkers, biologically active compounds, and economical aspects. In: Ulber, R., Le Gal, Y. (Eds.), *Marine Biotechnology I*. Springer, Berlin, Heidelberg, pp. 49–125. <https://doi.org/10.1007/b135782>.
- Bligh, E.G., Dyer, W.J., 1959. A rapid method of total lipid extraction and purification. *Can. J. Biochem. Physiol.* 37, 911–917. <https://doi.org/10.1139/o59-099>.
- Blighe, K., 2018. EnhancedVolcano. <https://doi.org/10.18129/B9.BIOC.ENHANCEDVOLCANO>.
- Bourdages, H.R., M. J., M.C., G. P., Isabel, L., 2022. Assessment of northern shrimp stocks in the Estuary and gulf of St. Lawrence in 2021: commercial fishery and research survey data. *DFO Can. Sci. Adv. Sec. Res. Doc.* 2022/027.
- Bourret, A., Leung, C., Puncher, G.N., Corre, N.L., Deslauriers, D., Skanes, K., Bourdages, H., Ros, M.C.-D., Walkusz, W., Jeffery, N.W., Stanley, R.R.E., Parent, G. J., 2024. Diving into broad-scale and high-resolution population genomics to decipher drivers of structure and climatic vulnerability in a marine invertebrate. <https://doi.org/10.1101/2024.01.29.577252>.
- Bozinovic, F., Calosi, P., Spicer, J.I., 2011. Physiological correlates of geographic range in animals. *Annu. Rev. Ecol. Syst.* 42, 155–179. <https://doi.org/10.1146/annurev-ecolsys-102710-145055>.
- Caldeira, K., Wickett, M.E., 2003. Anthropogenic carbon and ocean pH. *Nature* 425, 365. <https://doi.org/10.1038/425365a>.
- Calosi, P., De Wit, P., Thor, P., Dupont, S., 2016. Will life find a way? Evolution of marine species under global change. *Evol. Appl.* 9, 1035–1042. <https://doi.org/10.1111/eva.12418>.
- Calosi, P., Melatunan, S., Turner, L.M., Artioli, Y., Davidson, R.L., Byrne, J.J., Viant, M. R., Widdicombe, S., Rundle, S.D., 2017. Regional adaptation defines sensitivity to future ocean acidification. *Nat. Commun.* 8, 13994. <https://doi.org/10.1038/ncomms13994>.
- Carrier-Belleau, C., Drolet, D., McKindsey, C.W., Archambault, P., 2021. Environmental stressors, complex interactions and marine benthic communities' responses. *Sci. Rep.* 11, 4194. <https://doi.org/10.1038/s41598-021-83533-1>.
- Chemel, M., Noisette, F., Chabot, D., Guscelli, E., Leclerc, L., Calosi, P., 2020. Good news – bad news: combined ocean change drivers decrease survival but have no negative impact on nutritional value and organoleptic quality of the northern shrimp. *Front. Mar. Sci.* 7, 611. <https://doi.org/10.3389/fmars.2020.00611>.
- Cho, H., Seol, Y., Baik, S., Sung, B., Ryu, C.S., Kim, Y.J., 2022. Mono(2-ethylhexyl) phthalate modulates lipid accumulation and reproductive signaling in *Daphnia magna*. *Environ. Sci. Pollut. Res.* 29, 55639–55650. <https://doi.org/10.1007/s11356-022-19701-1>.
- Chown, S.L., Gaston, K.J., 2008. Macrophysiology for a changing world. *Proc. R. Soc. B Biol. Sci.* 275, 1469–1478. <https://doi.org/10.1098/rspb.2008.0137>.
- Chwastek, G., Surma, M.A., Rizk, S., Grosse, D., Lavrynenko, O., Rucińska, M., Jambor, H., Sáenz, J., 2020. Principles of membrane adaptation revealed through

- environmentally induced bacterial lipidome remodeling. *Cell Rep.* 32, 108165. <https://doi.org/10.1016/j.celrep.2020.108165>.
- Cohen, J., 1992. A power primer. *Psychol. Bull.* 112, 155–159. <https://doi.org/10.1037//0033-2909.112.1.155>.
- Costello, C., Cao, L., Gelcich, S., Cisneros-Mata, M.Á., Free, C.M., Froehlich, H.E., Golden, C.D., Ishimura, G., Maier, J., Macadam-Somer, I., Mangin, T., Melnychuk, M.C., Miyahara, M., de Moor, C.L., Naylor, R., Nøstbakken, L., Ojea, E., O'Reilly, E., Parma, A.M., Plantinga, A.J., Thilsted, S.H., Lubchenco, J., 2020. The future of food from the sea. *Nature* 588, 95–100. <https://doi.org/10.1038/s41586-020-2616-y>.
- Côté, I.M., Darling, E.S., Brown, C.J., 2016. Interactions among ecosystem stressors and their importance in conservation. *Proc. R. Soc. B Biol. Sci.* 283, 20152592. <https://doi.org/10.1098/rspb.2015.2592>.
- da Costa, E., Melo, T., Moreira, A.S.P., Alves, E., Domingues, P., Calado, R., Abreu, M.H., Domingues, M.R., 2015. Decoding bioactive polar lipid profile of the macroalgae *Codium tomentosum* from a sustainable IMTA system using a lipidomic approach. *Algal Res.* 12, 388–397. <https://doi.org/10.1016/j.algal.2015.09.020>.
- DFO, 2025. Fisheries Landings Value by Province Datasets.
- DFO, 2022a. 2021 assessment of northern shrimp on the eastern scotian shelf (SFAS 13–15). *Can. Sci. Advis. Sec. Sci. Advis. Rep.* 2022/033.
- DFO, 2022b. Assessment of northern shrimp stocks in the Estuary and gulf of st. Lawrence in 2021. *Can. Sci. Advis. Sec. Sci. Advis. Rep.* 2022/006.
- DFO, 2021. Assessment of northern shrimp (*Pandalus borealis*) and striped shrimp (*Pandalus montagu*) in the eastern and Western assessment zones, February 2021. *Can. Sci. Advis. Sec. Sci. Advis. Rep.* 2021/014.
- DFO, 2020. Oceanographic Conditions in the Atlantic Zone in 2019.
- DFO, 2016. An Assessment of Northern Shrimp (*Pandalus borealis*) in Shrimp Fishing Areas 4–6 and of Striped Shrimp (*Pandalus montagu*) in Shrimp Fishing Area 4 in 2016.
- Doney, S.C., Fabry, V.J., Feely, R.A., Kleypas, J.A., 2009. Ocean acidification: the other CO<sub>2</sub> problem. *Ann. Rev. Mar. Sci.* 1, 169–192. <https://doi.org/10.1146/annurev.marine.010908.163834>.
- Dreier, D.A., Bowden, J.A., Aristizabal-Henao, J.J., Denslow, N.D., Martyniuk, C.J., 2020. Ecotoxicology-lipidomics: an emerging concept to understand chemical-metabolic relationships in comparative fish models. *Comp. Biochem. Physiol., Part D: Genomics Proteomics* 36, 100742. <https://doi.org/10.1016/j.cbd.2020.100742>.
- Drozdowski, A., Horne, E., 2022. Strait of canso port model hindcast evaluation. *Can. Tech. Rep. Hydrogr. Ocean Sci.* 341.
- Dupont-Prinet, A., Pillet, M., Chabot, D., Hansen, T., Tremblay, R., Audet, C., 2013. Northern shrimp (*Pandalus borealis*) oxygen consumption and metabolic enzyme activities are severely constrained by hypoxia in the Estuary and gulf of st. Lawrence. *J. Exp. Mar. Biol. Ecol.* 448, 298–307. <https://doi.org/10.1016/j.jembe.2013.07.019>.
- Dymond, M.K., 2015. Mammalian phospholipid homeostasis: homeoviscous adaptation deconstructed by lipidomic data driven modelling. *Chem. Phys. Lipids* 191, 136–146. <https://doi.org/10.1016/j.chemphyslip.2015.09.003>.
- Eide, M., Goksøy, A., Yadetie, F., Gilabert, A., Bartosova, Z., Frøysa, H.G., Fallahi, S., Zhang, X., Blaser, N., Jonassen, I., Bruheim, P., Alendal, G., Brun, M., Porte, C., Karlsen, O.A., 2023. Integrative omics-analysis of lipid metabolism regulation by peroxisome proliferator-activated receptor  $\alpha$  and  $\beta$  agonists in Male Atlantic cod. *Front. Physiol.* 14. <https://doi.org/10.3389/fphys.2023.1129089>.
- El Babili, M., Bodennec, J., Carsol, M.A., Brichon, G., Zwengelstein, G., 1997. Effects of temperature and intracellular pH on the sphingomyelin metabolism in the gills of crab, *Carcinus maenas*. *Comp. Biochem. Physiol. B Biochem. Mol. Biol.* 117, 125–133. [https://doi.org/10.1016/S0305-0491\(96\)00322-7](https://doi.org/10.1016/S0305-0491(96)00322-7).
- Ermolenko, E.V., Sikorskaya, T.V., 2021. Lipidome of the reef-building coral *Acropora cerasalis*: changes under thermal stress. *Biochem. Systemat. Ecol.* 97, 104276. <https://doi.org/10.1016/j.bse.2021.104276>.
- Ernst, R., Ballweg, S., Levental, I., 2018. Cellular mechanisms of physicochemical membrane homeostasis. *Curr. Opin. Cell Biol.*, Membrane Trafficking 53, 44–51. <https://doi.org/10.1016/j.ccb.2018.04.013>.
- Ernst, R., Ejsing, C.S., Antonny, B., 2016. Homeoviscous adaptation and the regulation of membrane lipids. *J. Mol. Biol., Molecular Biology of Membrane Lipids* 428, 4776–4791. <https://doi.org/10.1016/j.jmb.2016.08.013>.
- Facchini, L., Losito, I., Cataldi, T.R.I., Palmisano, F., 2016. Ceramide lipids in alive and thermally stressed mussels: an investigation by hydrophilic interaction liquid chromatography-electrospray ionization fourier transform mass spectrometry. *J. Mass Spectrom.* 51, 768–781. <https://doi.org/10.1002/jms.3832>.
- Falch, E., 2023. Physico-chemical properties and nutrition of marine lipids. *Foods* 12, 4078. <https://doi.org/10.3390/foods12224078>.
- FAO, 2024. The state of world fisheries and aquaculture 2024. <https://doi.org/10.4060/cd0683en>.
- FAO, 2022. Fishery and Aquaculture Statistics – Yearbook 2022. FAO. <https://doi.org/10.4060/cd4312en>.
- Foo, S.A., Byrne, M., 2016. Acclimatization and adaptive capacity of marine species in a changing ocean. *Adv. Mar. Biol.* 74, 69–116. <https://doi.org/10.1016/bbs.2016.06.001>.
- Feugere, Lauric, Fernandes, Joana Filipa, Guscelli, Ella, Melo, Tânia, Aveiro, Susana, Chabot, Denis, Calado, Ricardo, Domingues, Rosário, Madeira, Diana, Calosi, Piero, 2025a. Phospholipidome profile of and metadata associated with the abdomen muscle of female Northern shrimp *Pandalus borealis* collected in the wild from four geographic origins in the Northwest Atlantic [dataset bundled publication]. PANGAEA. <https://doi.org/10.1594/PANGAEA.982557>.
- Feugere, Lauric, Fernandes, Joana Filipa, Guscelli, Ella, Melo, Tânia, Aveiro, Susana, Chabot, Denis, Calado, Ricardo, Domingues, Rosário, Madeira, Diana, Calosi, Piero, 2025b. Raw and recalibrated phospholipidome profile of the abdomen muscle of female Northern shrimp *Pandalus borealis* collected in the wild from four geographic origins in the Northwest Atlantic [dataset]. PANGAEA. In: Feugere, L et al. (2025): Phospholipidome profile of and metadata associated with the abdomen muscle of female Northern shrimp *Pandalus borealis* collected in the wild from four geographic origins in the Northwest Atlantic [dataset bundled publication]. PANGAEA. <https://doi.org/10.1594/PANGAEA.982562>. <https://doi.org/10.1594/PANGAEA.982557>.
- Feugere, Lauric, Fernandes, Joana Filipa, Guscelli, Ella, Melo, Tânia, Aveiro, Susana, Chabot, Denis, Calado, Ricardo, Domingues, Rosário, Madeira, Diana, Calosi, Piero, 2025c. Normalised phospholipidome profile of and metadata associated with the abdomen muscle of female Northern shrimp *Pandalus borealis* collected in the wild from four geographic origins in the Northwest Atlantic [dataset]. PANGAEA. In: Feugere, L et al. (2025): Phospholipidome profile of and metadata associated with the abdomen muscle of female Northern shrimp *Pandalus borealis* collected in the wild from four geographic origins in the Northwest Atlantic [dataset bundled publication]. PANGAEA. <https://doi.org/10.1594/PANGAEA.982561>. <https://doi.org/10.1594/PANGAEA.982557>.
- Frallicciardi, J., Melcr, J., Signou, P., Marrink, S.J., Poolman, B., 2022. Membrane thickness, lipid phase and sterol type are determining factors in the permeability of membranes to small solutes. *Nat. Commun.* 13, 1605. <https://doi.org/10.1038/s41467-022-29272-x>.
- Fuertes, I., Piña, B., Barata, C., 2020. Changes in lipid profiles in *Daphnia magna* individuals exposed to low environmental levels of neuroactive pharmaceuticals. *Sci. Total Environ.* 733, 139029. <https://doi.org/10.1016/j.scitotenv.2020.139029>.
- Garcia, E.G., 2007. The northern shrimp (*Pandalus borealis*) offshore fishery in the northeast Atlantic. In: *Advances in Marine Biology*. Elsevier, pp. 147–266. [https://doi.org/10.1016/S0065-2881\(06\)52002-4](https://doi.org/10.1016/S0065-2881(06)52002-4).
- Garzke, J., Hansen, T., Ismar, S.M.H., Sommer, U., 2016. Combined effects of ocean warming and acidification on copepod abundance, body size and fatty acid content. *PLoS One* 11, e0155952. <https://doi.org/10.1371/journal.pone.0155952>.
- Gaston, K.J., Chown, S.L., Calosi, P., Bernardo, J., Bilton, D.T., Clarke, A., Clusella-Trullas, S., Ghalambor, C.K., Konarzewski, M., Peck, L.S., Porter, W.P., Pörtner, H.O., Rezende, E.L., Schulte, P.M., Spicer, J.I., Stillman, J.H., Terblanche, J.S., Van Kleunen, M., 2009. Macrophysiology: a conceptual reification. *Am. Nat.* 174, 595–612. <https://doi.org/10.1086/605982>.
- Gibb, O., Cyr, F., Azetsu-Scott, K., Chassé, J., Galbraith, P.S., Maillet, G., Pepin, P., Punshon, S., Starr, M., 2023. Spatiotemporal variability of pH and carbonate parameters on the Canadian Atlantic Continental shelf between 2014 and 2020. <https://doi.org/10.5194/essd-2022-460>.
- Gillett, R.D., 2008. Global Study of Shrimp Fisheries, FAO Fisheries Technical Paper. FAO, Rome.
- Guscelli, E., 2024. Sensibilité des populations de crevette nordique aux changements globaux le long de la côte est du Canada. Université de Québec à Rimouski. Département De Biologie, Chimie Et Géographie.
- Guscelli, E., Chabot, D., Vermandele, F., Madeira, R., Calosi, P., 2023a. All roads lead to rome: inter-origin variation in metabolomics reprogramming of the northern shrimp exposed to global changes leads to a comparable physiological status. *Front. Mar. Sci.* 10. <https://doi.org/10.3389/fmars.2023.1170451>.
- Guscelli, E., Noisette, F., Chabot, D., Blier, P.U., Hansen, T., Cassista-Da Ros, M., Pepin, P., Skanes, K.R., Calosi, P., 2024. Seawater parameters during the experiments with multiple populations of the northern shrimp (*Pandalus borealis*) exposed to global change drivers. <https://doi.org/10.1594/PANGAEA.966793>.
- Guscelli, E., Noisette, F., Chabot, D., Blier, P.U., Hansen, T., Cassista-Da Ros, M., Pepin, P., Skanes, K.R., Calosi, P., 2023b. Northern shrimp from multiple origins show similar sensitivity to global change drivers, but different cellular energetic capacity. *J. Exp. Biol.* 226, jeb245400. <https://doi.org/10.1242/jeb.245400>.
- Han, X., Gross, R.W., 2022. The foundations and development of lipidomics. *J. Lipid Res.* 63. <https://doi.org/10.1016/j.jlr.2021.100164>.
- Han, X., Gross, R.W., 2003. Global analyses of cellular lipidomes directly from crude extracts of biological samples by ESI mass spectrometry: a bridge to lipidomics. *J. Lipid Res.* 44, 1071–1079. <https://doi.org/10.1194/jlr.R300004-JLR200>.
- Hazel, J., 1990. The role of alterations in membrane lipid composition in enabling physiological adaptation of organisms to their physical environment. *Prog. Lipid Res.* 29, 167–227. [https://doi.org/10.1016/0163-7827\(90\)90002-3](https://doi.org/10.1016/0163-7827(90)90002-3).
- Hazel, J.R., 1995. Thermal adaptation in biological membranes: is homeoviscous adaptation the explanation? *Annu. Rev. Physiol.* 57, 19–42. <https://doi.org/10.1146/annurev.ph.57.030195.000315>.
- Holm, H.C., Fredricks, H.F., Bent, S.M., Lowenstein, D.P., Ossolinski, J.E., Becker, K.W., Johnson, W.M., Schrage, K., Van Mooy, B.A.S., 2022. Global ocean lipidomes show a universal relationship between temperature and lipid unsaturation. *Science* 376, 1487–1491. <https://doi.org/10.1126/science.abn7455>.
- Horton, B.P., Khan, N.S., Cahill, N., Lee, J.S.H., Shaw, T.A., Garner, A.J., Kemp, A.C., Engelhart, S.E., Rahmstorf, S., 2020. Estimating global mean sea-level rise and its uncertainties by 2100 and 2300 from an expert survey. *Npj Clim. Atmospheric Sci.* 3, 1–8. <https://doi.org/10.1038/s41612-020-0121-5>.
- Imbs, A.B., Ermolenko, E.V., Grigorchuk, V.P., Sikorskaya, T.V., Velansky, P.V., 2021. Current progress in lipidomics of marine invertebrates. *Mar. Drugs* 19, 660. <https://doi.org/10.3390/md19120660>.

- IPCC, 2022. The Ocean and Cryosphere in a Changing Climate: Special Report of the Intergovernmental Panel on Climate Change, first ed. Cambridge University Press. <https://doi.org/10.1017/9781009157964>.
- Jin, P., Liang, Z., Overmans, S., Xia, J., 2021. Lipid remodeling reveals the adaptations of a marine diatom to ocean acidification. *Front. Microbiol.* 12. <https://doi.org/10.3389/fmicb.2021.748445>.
- Johnson, W.T., Dorn, N.C., Ogbonna, D.A., Bottini, N., Shah, N.J., 2021. Lipid-based regulators of immunity. *Bioeng. Transl. Med.* 7, e10288. <https://doi.org/10.1002/btm2.10288>.
- Käkelä, R., Mattila, M., Hermansson, M., Haimi, P., Uphoff, A., Pajanen, V., Somerharju, P., Vornanen, M., 2008. Seasonal acclimatization of brain lipidome in a eurythermal fish (*Carassius carassius*) is mainly determined by temperature. *Am. J. Physiol. Regul. Integr. Comp. Physiol.* 294, R1716–R1728. <https://doi.org/10.1152/ajpregu.00883.2007>.
- Koeller, P., Covey, M., King, M., 2007. Biological and environmental requisites for a successful trap fishery of the Northern shrimp *Pandalus borealis*. *Proc. Nova Scotian Inst. Sci. NSIS* 44. <https://doi.org/10.15273/pnsis.v44i1.3882>.
- Koelmel, J.P., Napolitano, M.P., Ulmer, C.Z., Vasiliou, V., Garrett, T.J., Yost, R.A., Prasad, M.N.V., Godri Pollitt, K.J., Bowden, J.A., 2020. Environmental lipidomics: understanding the response of organisms and ecosystems to a changing world. *Metabolomics* 16, 56. <https://doi.org/10.1007/s11306-020-01665-3>.
- Kučerka, N., Nieh, M.-P., Katsaras, J., 2011. Fluid phase lipid areas and bilayer thicknesses of commonly used phosphatidylcholines as a function of temperature. *Biochim. Biophys. Acta BBA - Biomembr.* 1808, 2761–2771. <https://doi.org/10.1016/j.bbame.2011.07.022>.
- Kyle, J.E., Aimo, L., Bridge, A.J., Clair, G., Fedorova, M., Helms, J.B., Molenaar, M.R., Ni, Z., Orešić, M., Slenker, D., Willighagen, E., Webb-Robertson, B.-J.M., 2021. Interpreting the lipidome: bioinformatic approaches to embrace the complexity. *Metabolomics* 17, 55. <https://doi.org/10.1007/s11306-021-01802-6>.
- Latyshov, N.A., Kasyanov, S.P., Kharlamenko, V.I., Svetashev, V.I., 2009. Lipids and of fatty acids of edible crabs of the north-western Pacific. *Food Chem.* 116, 657–661. <https://doi.org/10.1016/j.foodchem.2009.02.085>.
- Lenth, R.V., 2024. *Emmeans: estimated marginal means. Aka Least-Squares Means*.
- Leo, E., Graeve, M., Storch, D., Pörtner, H.-O., Mark, F.C., 2020. Impact of ocean acidification and warming on mitochondrial enzymes and membrane lipids in two gadoid species. *Polar Biol.* 43, 1109–1120. <https://doi.org/10.1007/s00300-019-02600-6>.
- Leung, C., Guscetti, E., Chabot, D., Bourret, A., Calosi, P., Parent, G.J., 2023. The lack of genetic variation underlying thermal transcriptomic plasticity suggests limited adaptability of the northern shrimp, *Pandalus borealis*. *Front. Ecol. Evol.* 11, 1125134. <https://doi.org/10.3389/fevo.2023.1125134>.
- Liebisch, G., Fahy, E., Aoki, J., Dennis, E.A., Durand, T., Ejsing, C.S., Fedorova, M., Feussner, I., Griffiths, W.J., Köfeler, H., Merrill, A.H., Murphy, R.C., O'Donnell, V.B., Oskolkova, O., Subramaniam, S., Wakelam, M.J.O., Spener, F., 2020. Update on LIPID MAPS classification, nomenclature, and shorthand notation for MS-derived lipid structures. *J. Lipid Res.* 61, 1539–1555. <https://doi.org/10.1194/jlr.S120001025>.
- Lischka, S., Greenacre, M.J., Riebesell, U., Graeve, M., 2022. Membrane lipid sensitivity to ocean warming and acidification poses a severe threat to arctic pteropods. *Front. Mar. Sci.* 9. <https://doi.org/10.3389/fmars.2022.920163>.
- Lordan, R., Tsoupras, A., Zabetakis, I., 2017. Phospholipids of animal and marine origin: structure, function, and anti-inflammatory properties. *Mol. J. Synth. Chem. Nat. Prod. Chem.* 22, 1964. <https://doi.org/10.3390/molecules22111964>.
- Madeira, D., Araújo, J.E., Vitorino, R., Costa, P.M., Capelo, J.L., Vinagre, C., Diniz, M.S., 2017. Molecular plasticity under ocean warming: proteomics and fitness data provides clues for a better understanding of the thermal tolerance in fish. *Front. Physiol.* 8. <https://doi.org/10.3389/fphys.2017.00825>.
- Madeira, D., Madeira, C., Calosi, P., Vermandele, F., Carrier-Belleau, C., Barria-Araya, A., Daigle, R., Findlay, H.S., Poisot, T., 2024. Multilayer biological networks to upscale marine research to global change-smart management and sustainable resource use. *Sci. Total Environ.* 944, 173837. <https://doi.org/10.1016/j.scitotenv.2024.173837>.
- Malekar, V.C., Morton, J.D., Hider, R.N., Cruickshank, R.H., Hodge, S., Metcalf, V.J., 2018. Effect of elevated temperature on membrane lipid saturation in antarctic notothenioid fish. *PeerJ* 6, e4765. <https://doi.org/10.7717/peerj.4765>.
- Mangiafico, S.S., 2024. *Recompianion: functions to support extension education program evaluation. Rutgers Cooperative Extension. New Brunswick, New Jersey*.
- Meek, M.H., Beever, E.A., Barbosa, S., Fitzpatrick, S.W., Fletcher, N.K., Mittan-Moreau, C.S., Reid, B.N., Campbell-Staton, S.C., Green, N.F., Hellmann, J.J., 2023. Understanding local adaptation to prepare populations for climate change. *Bioscience* 73, 36–47. <https://doi.org/10.1093/biosci/biac101>.
- Melo, T., Alves, E., Azevedo, V., Martins, A.S., Neves, B., Domingues, P., Calado, R., Abreu, M.H., Domingues, M.R., 2015. Lipidomics as a new approach for the bioprospecting of marine macroalgae — unraveling the polar lipid and fatty acid composition of *Chondrus crispus*. *Algal Res.* 8, 181–191. <https://doi.org/10.1016/j.algal.2015.02.016>.
- Mesmar, F., Muhsen, M., Farooq, I., Maxey, G., Tourigny, J.P., Tennessen, J., Bondesson, M., 2024. Exposure to the pesticide tefluthrin causes developmental neurotoxicity in zebrafish. <https://doi.org/10.1101/2024.05.28.596249>.
- Mika, A., Skorkowski, E., Stepnowski, P., Golebiowski, M., 2013. The lipid composition of the abdominal muscle of shrimp crangon crangon from the gulf of gdansk in spring and winter periods. *J. Mar. Biol. Assoc. U. K.* 93, 1825–1833. <https://doi.org/10.1017/S002531541300057X>.
- Mimura, M., Yahara, T., Faith, D.P., Vázquez-Domínguez, E., Colautti, R.I., Araki, H., Javadi, F., Núñez-Farfán, J., Mori, A.S., Zhou, S., Hollingsworth, P.M., Neves, L.E., Fukano, Y., Smith, G.F., Sato, Y., Tachida, H., Hendry, A.P., 2017. Understanding and monitoring the consequences of human impacts on intraspecific variation. *Evol. Appl.* 10, 121–139. <https://doi.org/10.1111/eva.12436>.
- Mohamed, A., Molendijk, J., 2023. Lipidr: data mining and analysis of lipidomics datasets. <https://doi.org/10.18129/B9.bioc.lipidr>.
- Molenaar, M.R., Haaker, M.W., Vaandrager, A.B., Houweling, M., Helms, J.B., 2023. Lipidomic profiling of rat hepatic stellate cells during activation reveals a two-stage process accompanied by increased levels of lysosomal lipids. *J. Biol. Chem.* 299, 103042. <https://doi.org/10.1016/j.jbc.2023.103042>.
- Molenaar, M.R., Jeucken, A., Wassenaar, T.A., van de Lest, C.H.A., Brouwers, J.F., Helms, J.B., 2019. LION/web: a web-based ontology enrichment tool for lipidomic data analysis. *GigaScience* 8, giz061. <https://doi.org/10.1093/gigascience/giz061>.
- Mucci, A., Levasseur, M., Gratton, Y., Martias, C., Scarratt, M., Gilbert, D., Tremblay, J.-É., Ferreyra, G., Lansard, B., 2018. Tidally induced variations of pH at the head of the Laurentian channel. *Can. J. Fish. Aquat. Sci.* 75, 1128–1141. <https://doi.org/10.1139/cjfas-2017-0007>.
- Mucci, A., Starr, M., Gilbert, D., Sundby, B., 2011. Acidification of lower St. Lawrence Estuary bottom waters. *Atmos.-Ocean* 49, 206–218. <https://doi.org/10.1080/07055900.2011.599265>.
- Muff, S., Nilsen, E.B., O'Hara, R.B., Nater, C.R., 2022. Rewriting results sections in the language of evidence. *Trends Ecol. Evol.* 37, 203–210. <https://doi.org/10.1016/j.tree.2021.10.009>.
- Muir, A.P., Nunes, F.L.D., Dubois, S.F., Pernet, F., 2016. Lipid remodelling in the reef-building honeycomb worm, *Sabellaria alveolata*, reflects acclimation and local adaptation to temperature. *Sci. Rep.* 6, 35669. <https://doi.org/10.1038/srep35669>.
- Muzić, T., Tounsi, F., Madsen, S.B., Pollakowski, D., Konrad, M., Heimburg, T., 2019. Melting transitions in biomembranes. *Biochim. Biophys. Acta BBA - Biomembr.* 1861, 183026. <https://doi.org/10.1016/j.bbame.2019.07.014>.
- Noisette, F., Calosi, P., Madeira, D., Chemel, M., Menu-Courey, K., Piedalue, S., Gurney-Smith, H., Daoud, D., Azetsu-Scott, K., 2021. Tolerant larvae and sensitive juveniles: integrating metabolomics and whole-organism responses to define life-stage specific sensitivity to ocean acidification in the American lobster. *Metabolites* 11, 584. <https://doi.org/10.3390/metabol11090584>.
- Ohtsu, T., Kimura, M.T., Katagiri, C., 1998. How drosophila species acquire cold tolerance. *Eur. J. Biochem.* 252, 608–611. <https://doi.org/10.1046/j.1432-1327.1998.2520608.x>.
- Ouellet, P., Chabot, D., Calosi, P., Orr, D., Galbraith, P.S., 2017. Regional variations in early life stages response to a temperature gradient in the northern shrimp *Pandalus borealis* and vulnerability of the populations to ocean warming. *J. Exp. Mar. Biol. Ecol.* 497, 50–60. <https://doi.org/10.1016/j.jembe.2017.09.007>.
- Patton, J.L., Srinivasan, B., Dickson, R.C., Lester, R.L., 1992. Phenotypes of sphingolipid-dependent strains of *Saccharomyces cerevisiae*. *J. Bacteriol.* 174, 7180–7184. <https://doi.org/10.1128/jb.174.22.7180-7184.1992>.
- Perez-Velazquez, M., González-Félix, M.L., Lawrence, A.L., Gatlin III, D.M., 2003. Changes in lipid class and fatty acid composition of adult male *Litopenaeus vannamei* (Boone) in response to culture temperature and food deprivation. *Aquac. Res.* 34, 1205–1213. <https://doi.org/10.1046/j.1365-2109.2003.00931.x>.
- Piggott, J.J., Townsend, C.R., Matthaie, C.D., 2015. Reconceptualizing synergism and antagonism among multiple stressors. *Ecol. Evol.* 5, 1538–1547. <https://doi.org/10.1002/ece3.1465>.
- Rey, F., Melo, T., Lopes, D., Couto, D., Marques, F., Domingues, M.R., 2022. Applications of lipidomics in marine organisms: progress, challenges and future perspectives. *Mol. Omics* 18, 357–386. <https://doi.org/10.1039/D2MO00012A>.
- Richards, R.A., Hunter, M., 2021. Northern shrimp *Pandalus borealis* population collapse linked to climate-driven shifts in predator distribution. *PLoS One* 16, e0253914. <https://doi.org/10.1371/journal.pone.0253914>.
- Ritchie, M.E., Phipson, B., Wu, D., Hu, Y., Law, C.W., Shi, W., Smyth, G.K., 2015. Limma powers differential expression analyses for RNA-seq and microarray studies. *Nucleic Acids Res.* 43, e47. <https://doi.org/10.1093/nar/gkv007>.
- Rivest, E.B., Hofmann, G.E., 2015. Effects of temperature and pCO<sub>2</sub> on lipid use and biological parameters of planulae of *Pocillopora damicornis*. *J. Exp. Mar. Biol. Ecol.* 473, 43–52. <https://doi.org/10.1016/j.jembe.2015.07.015>.
- Robles-Romo, A., Zenteno-Savín, T., Racotta, I.S., 2016. Bioenergetic status and oxidative stress during escape response until exhaustion in whiteleg shrimp *Litopenaeus vannamei*. *J. Exp. Mar. Biol. Ecol.* 478, 16–23. <https://doi.org/10.1016/j.jembe.2016.01.016>.
- Schmidt, E., Donelson, J.M., 2024. Regional thermal variation in a coral reef fish. *Conserv. Physiol.* 12, coae058. <https://doi.org/10.1093/conphys/coae058>.
- Schoepf, V., Grotoli, A.G., Warner, M.E., Cai, W.-J., Melman, T.F., Hoadley, K.D., Pettay, D.T., Hu, X., Li, Q., Xu, H., Wang, Y., Matsui, Y., Baumann, J.H., 2013. Coral energy reserves and calcification in a High-CO<sub>2</sub> world at two temperatures. *PLoS One* 8, e75049. <https://doi.org/10.1371/journal.pone.0075049>.
- Shumway, S.E., 1985. *Synopsis of Biological Data on the Pink Shrimp, vol. 1838. Pandalus borealis Krøyer*.
- Sikorskaya, T.V., Ermolenko, E.V., Imbs, A.B., 2020. Effect of experimental thermal stress on lipidomes of the soft coral *Sinularia* sp. and its symbiotic dinoflagellates. *J. Exp. Mar. Biol. Ecol.* 524, 151295. <https://doi.org/10.1016/j.jembe.2019.151295>.
- Sinensky, M., 1974. Homeoviscous Adaptation—A homeostatic process that regulates the viscosity of membrane lipids in *Escherichia coli*. *Proc. Natl. Acad. Sci. U. S. A.* 71, 522–525.

- Smit, M.G.D., Bechmann, R.K., Hendriks, A.J., Skadsheim, A., Larsen, B.K., Baussant, T., Bamber, S., Sanni, S., 2009. Relating biomarkers to whole-organism effects using species sensitivity distributions: a pilot study for marine species exposed to oil. *Environ. Toxicol. Chem.* 28 (1), 1104–1109. <https://doi.org/10.1897/08-464>.
- Swinnen, J.V., Dehairs, J., 2022. A beginner's guide to lipidomics. *Biochemist* 44, 20–24. [https://doi.org/10.1042/bio.2021\\_181](https://doi.org/10.1042/bio.2021_181).
- Tang, C.-H., Shi, S.-H., Lin, C.-Y., Li, H.-H., Wang, W.-H., 2019. Using lipidomic methodology to characterize coral response to herbicide contamination and develop an early biomonitoring model. *Sci. Total Environ.* 648, 1275–1283. <https://doi.org/10.1016/j.scitotenv.2018.08.296>.
- Thor, P., Bailey, A., Dupont, S., Calosi, P., Søreide, J.E., De Wit, P., Guscelli, E., Loubet-Sartrou, L., Deichmann, I.M., Candee, M.M., Svensen, C., King, A.L., Bellerby, R.G.J., 2018. Contrasting physiological responses to future ocean acidification among arctic copepod populations. *Glob. Change Biol.* 24, e365–e377. <https://doi.org/10.1111/gcb.13870>.
- Trautenberg, L.C., Brankatschk, M., Shevchenko, A., Wigby, S., Reinhardt, K., 2022. Ecological lipidology. *eLife* 11, e79288. <https://doi.org/10.7554/eLife.79288>.
- Valles-Regino, R., Tate, R., Kelaher, B., Savins, D., Dowell, A., Benkendorff, K., 2015. Ocean warming and CO<sub>2</sub>-induced acidification impact the lipid content of a marine predatory gastropod. *Mar. Drugs* 13, 6019–6037. <https://doi.org/10.3390/md13106019>.
- Vásquez, C., Quiñones, R.A., Brante, A., Hernández-Miranda, E., 2023. Genetic diversity and resilience in benthic marine populations. *Rev. Chil. Hist. Nat.* 96, 4. <https://doi.org/10.1186/s40693-023-00117-1>.
- Wan, L., Peng, Yingying, Yu, Huaihua, Xu, Wenjun, He, J., 2022. Comparing the muscle nutritional quality of eight common wild-caught economic shrimp species from the East China Sea. *J. Aquat. Food Prod. Technol.* 31, 549–564. <https://doi.org/10.1080/10498850.2022.2081062>.
- Wassenaar, T.A., Ingólfsson, H.I., Böckmann, R.A., Tieleman, D.P., Marrink, S.J., 2015. Computational lipidomics with insane: a versatile tool for generating custom membranes for molecular simulations. *J. Chem. Theor. Comput.* 11, 2144–2155. <https://doi.org/10.1021/acs.jctc.5b00209>.
- Wickham, H., 2016. *ggplot2: Elegant Graphics for Data Analysis*. Springer-Verlag, New York.
- Winnikoff, J.R., Milshteyn, D., Vargas-Urbano, S.J., Pedraza, M.A., Armando, A.M., Quehenberger, O., Sodt, A., Gillilan, R.E., Dennis, E.A., Lyman, E., Haddock, S.H.D., Budin, I., 2024. Homeocurvature adaptation of phospholipids underlies pressure-specialization of deep-sea invertebrates. *Science* 384, 1482–1488. <https://doi.org/10.1126/science.adm7607>.
- Wood, P.L., Wood, M.D., Kunigelis, S.C., 2023. Pilot lipidomics study of copepods: investigation of potential lipid-based biomarkers for the early detection and quantification of the biological effects of climate change on the Oceanic food chain. *Life* 13, 2335. <https://doi.org/10.3390/life13122335>.
- Xianlin, H., 2016. Lipids and lipidomics. In: *Lipidomics*. John Wiley & Sons, Ltd, pp. 1–20. <https://doi.org/10.1002/9781119085263.ch1>.
- Yan, L., 2023. *ggvenn: Draw Venn Diagram by "ggplot2"*.
- Yu, Z.-L., Li, D.-Y., Yin, F.-W., Zhao, Q., Liu, Z.-Y., Song, L., Zhou, D.-Y., Wang, T., 2020. Lipid profiles in By-Products and muscles of three shrimp species (*Penaeus monodon*, *Penaeus vannamei*, and *Penaeus chinensis*). *Eur. J. Lipid Sci. Technol.* 122, 1900309. <https://doi.org/10.1002/ejlt.201900309>.
- DFO, 2024. Rebuilding plan: Northern shrimp (*Pandalus borealis*) - Shrimp fishing area 6. [https://www.dfo-mpo.gc.ca/fisheries-peches/ifmp-gmp/shrimp-crevette/sfa6-zpc6-2024-eng.html#\\_Toc181092862/](https://www.dfo-mpo.gc.ca/fisheries-peches/ifmp-gmp/shrimp-crevette/sfa6-zpc6-2024-eng.html#_Toc181092862/) (accessed 28 March 2025).